AUTOCALIBRATION OF CAMERAS WITH KNOWN PIXEL SHAPE

JOSÉ I. RONDA*, ANTONIO VALDÉS**, AND GUILLERMO GALLEGO*

Abstract. We present new algorithms for the recovery of the Euclidean structure from a projective calibration of a set of cameras of known pixel shape but otherwise arbitrarily varying intrinsic and extrinsic parameters. The algorithms have a geometrical motivation based on the properties of the set of lines intersecting the absolute conic. The theoretical part of the paper contributes with theoretical results that establish the relationship between the geometrical object corresponding to this set of lines and other equivalent objects as the absolute quadric. Finally, the satisfactory performance of the techniques is demonstrated with synthetic and real data.

* Grupo de Tratamiento de Imágenes
Universidad Politécnica de Madrid
E-28040 Madrid, Spain
{jir,ggb}@gti.ssr.upm.es

** Dep. de Geometría y Topología
Universidad Complutense de Madrid
E-28040 Madrid, Spain
Antonio_Valdes@mat.ucm.es

1. Introduction

As is well known, a standard strategy to solve the structure from motion problem when the intrinsic parameters of the cameras are unknown relies on a two-step process [5]. In the first step, a projective reconstruction of the scene is obtained, and, in the second, this reconstruction is upgraded to a Euclidean reconstruction in an operation that also provides the camera intrinsic parameters. This second step requires some restrictions in the internal parameters of the cameras, such as their constancy or the knowledge of some of their values. The specific problem of determining the camera internal parameters exclusively from the apparent motion of objects in the images is known as camera autocalibration.

Euclidean upgrading techniques usually have a geometrical motivation, steming from the fact that identifying a Euclidean structure in a projective space consists in locating

Date: July 28, 2005.
This work has been partly supported by the Comisión Interministerial de Ciencia y Tecnología (CICYT) of the Spanish Government.

the plane at infinity and the absolute conic lying in this plane and this in turn is equivalent to camera autocalibration [5]. Consequently, most autocalibration algorithms are based on techniques to obtain either the position of the absolute conic in the projectively reconstructed scene or its projection onto the image planes.

The possibility of autocalibrating a set of cameras with constant intrinsic parameters was shown for the first time in the modern computer vision literature in [9]. Since then, different techniques have been developed to cope with different practical situations. The case of varying intrinsic parametes has been studied in different works. In [7] the possibility of performing autocalibration in the case of square pixels and otherwise arbitrarily varying parameters is shown, and an algorithm is provided that aims at minimizing the reprojection error with the camera intrinsic and extrinsic parameters as variables. In [10] an algorithm based on the optimization of a cost function depending on the *dual absolute quadric* (DAQ) [16] and the intrinsic camera parameters. [15] proposes an iterative method to improve an initial guess in the principal point position. In [1] rotating cameras are considered, employing restrictions in the intrinsic parameters to obtain linear equations. For a survey on the subject we refer to [6].

There exist two geometrical objects that, being equivalent to the absolute conic, are easier to handle. The first one is the aforementioned DAQ, consisting in the set of planes tangent to the absolute conic. The second is the the *absolute line quadric* (ALQ), given by the set of lines that intersect the absolute conic. A 6×6 symmetric matrix which can be proved to be equivalent to the ALQ appeared in [11], resulting from an elaboration on the characterization of zero-skew perspective projection matrices [8][10]. Among other results, [11] proposes a parametrization of the space of such symmetric matrices and linear and non-linear autocalibration algorithms for the case of zero-skew cameras. Mathematical properties of the ALQ have been studied in [17, 18] using algebraic geometry and exterior algebra techniques. Some geometric aspects of the ALQ are also studied in [12].

In this paper we present new properties of the ALQ, exploiting them to obtain new autocalibration algorithms. The presentation is self-contained, including the description of the ALQ by means of Plücker coordinates and matrix algebra techniques. The new results include closed-form expressions for the camera intrinsic parameters from the ALQ, the obtainment of the DAQ from the ALQ using straightforward matrix operations, and an equally directcomputation of a Euclidean-upgrading homography.

In the experimental part of this work the different algorithmic possibilities arising from the ALQ are systematically explored and analyzed in terms of efficiency and computational cost. In particular, the potencial of the ALQ to provide accurate initializations will be exploited, which is a differentiating property from other approaches. Experiments of reconstruction with real data are provided.

The paper is organized as follows. Section 2 introduces the autocalibration problem, with emphasis in the case of cameras with known pixel shape. Section 3 introduces Plücker coordinates with all the necessary results and details. Then section 4 introduces the ALQ in a new way that makes explicit its relationship with the absolute quadric. The new autocalibration techniques that arise from this work are presented with simulation results in section 6 and tested with real data in section 7.

2. Problem formulation and motivation of the approach

We will assume that the camera can be modeled [5] by the usual linear equation $\mathbf{x} \sim \mathtt{P}\mathbf{X}$, where $\sim$ means equality up to a non-zero scale factor, $\mathbf{X} = (X, Y, Z, T)^\top$ denotes the homogeneous coordinates of a spatial point, $\mathbf{x} = (u, v, w)^\top$ represents the homogeneous coordinates of an image point, and $\mathtt{P}$ is the 3×4 matrix $\mathtt{P} = \mathtt{K}(\mathtt{R}| - \mathtt{R}\mathbf{t})$. The intrinsic parameter matrix $\mathtt{K}$ is given by

$$\mathtt{K} = \begin{pmatrix} \alpha_u & -\alpha_u \cot\theta & u_0 \\ 0 & \alpha_v / \sin\theta & v_0 \\ 0 & 0 & 1 \end{pmatrix}, \tag{1}$$

where u_0 and v_0 are the affine coordinates of the principal point, α_u and α_v are the pixel scale factors and θ is the skew angle between the axes of the pixel coordinates. We denote by $\tau = \alpha_u/\alpha_v$ the pixel aspect ratio. The matrix $\mathtt{R}$ is a rotation matrix which gives the camera orientation, and $\mathbf{t}$ are the coordinates of the camera center.

As is well known [5], it is possible to obtain a projective calibration only from point correspondences within two or more images. This means that, given a set of projected points $\mathbf{x}_{ij}$ obtained with N cameras, $N \geq 2$, we can obtain a set of matrices $\hat{\mathtt{P}}_i$ and a set of point coordinates $\hat{\mathbf{X}}_j$ such that $\mathbf{x}_{ij} \sim \hat{\mathtt{P}}_i \hat{\mathbf{X}}_j$, where $\hat{\mathtt{P}}_i = \mathtt{P}_i \mathtt{H}^{-1}$ and $\hat{\mathbf{X}}_j = \mathtt{H}\mathbf{X}_j$ for some non-singular 4×4 matrix $\mathtt{H}$.

Euclidean calibration can be defined as the obtainment of a matrix $\mathtt{H}$ changing the projective coordinates of a given projective calibration to some Euclidean coordinate system, i.e., one in which the absolute conic has equations $X^2 + Y^2 + Z^2 = T = 0$ [14].

3. Line representation

Plücker coordinates are a very convenient mathematical representation of the lines in 3D space. The core of Plücker theory is the existence of two natural one-to-one correspondances between lines of space and the set of rank-two 4×4 antisymmetric matrices. In this section we summarize the notation and results of Plücker theory that will be relevant in the rest of the paper, with proofs left for the appendix. References for line geometry are [13, 14].

3.1. **Plücker matrices.** Given two vectors $\mathbf{u} = (u_0, u_1, u_2, u_3)^\top$, $\mathbf{v} = (v_0, v_1, v_2, v_3)^\top$ $\in \mathbb{C}^4$, we define the antisymmetric matrix

$$\mathtt{M}(\mathbf{u},\mathbf{v}) = \mathbf{u}\mathbf{v}^\top - \mathbf{v}\mathbf{u}^\top = \begin{pmatrix} 0 & m_{01} & m_{02} & m_{03} \\ -m_{01} & 0 & m_{12} & m_{13} \\ -m_{02} & -m_{12} & 0 & m_{23} \\ -m_{03} & -m_{13} & -m_{23} & 0 \end{pmatrix} \tag{2}$$

where $m_{ij} = u_i v_j - u_j v_i$. If $\mathbf{u}$ and $\mathbf{v}$ are linearly independent, $\mathtt{M}(\mathbf{u},\mathbf{v})$ is a rank-two matrix, and otherwise it vanishes (see appendix A.1, P1).

Given points $\mathbf{p}$, $\mathbf{q}$ defining the line l, we define the *P-matrix* of l as

$$\mathrm{P} = \mathtt{M}(\mathbf{p}, \mathbf{q}). \tag{3}$$

The representation $l \mapsto \mathrm{P}$ is defined up to a non-zero scale factor (A.1, P2). A line is characterized by its P-matrix P, since the pencil of planes $\boldsymbol{\alpha}$ including the line is given (A.1, P3) by equation

$$\mathrm{P}\boldsymbol{\alpha} = 0. \tag{4}$$

Since P-matrices are singular, they verify

$$\det \mathrm{P} = (m_{01}m_{23} + m_{02}m_{31} + m_{03}m_{12})^2 = 0. \tag{5}$$

Conversely, any 4×4 non-zero antisymmetric matrix meeting this constraint turns out to be the P-matrix of some line (A.1, P4).

P-matrices also provide a straightforward way to compute the point $\mathbf{X}$ of intersection of a line l and a plane $\boldsymbol{\alpha}$ by means of the rule (A.1, P5)

$$\mathbf{X} = \mathrm{P}\boldsymbol{\alpha}. \tag{6}$$

We define the *Π-matrix* of a line given by two planes $\boldsymbol{\alpha}$ and $\boldsymbol{\beta}$ as the antisymmetric matrix

$$\Pi = \mathtt{M}(\boldsymbol{\alpha}, \boldsymbol{\beta}). \tag{7}$$

The properties of this matrix are dual versions of those of P-matrices. In particular, the Π-matrix of a line is uniquely defined up to scale by equation (7), that establishes another one-to-one mapping between the set of lines of space and the set of singular 4×4 non-null antisymmetric matrices, considered equal up to scale. Π-matrices characterize the set of points of the line by the relation $\Pi\mathbf{X} = 0$, and the plane $\boldsymbol{\gamma}$ defined by the line and an external point $\mathbf{X}$ is obtained as $\boldsymbol{\gamma} = \Pi\mathbf{X}$. We will term the P-matrix and the Π-matrix of a line as its *Plücker matrices.*

We also define, for two vectors $\mathbf{u}, \mathbf{v} \in \mathbb{C}^4$, the matrix $\mathtt{M}^*(\mathbf{u}, \mathbf{v})$ as the only one with the property

$$\mathbf{x}^\top \mathtt{M}^*(\mathbf{u}, \mathbf{v})\mathbf{y} = \det(\mathbf{x}, \mathbf{u}, \mathbf{v}, \mathbf{y}), \tag{8}$$

for any vectors $\mathbf{x}$, $\mathbf{y}$. Its explicit expression is

$$\mathtt{M}^*(\mathbf{u}, \mathbf{v}) = \begin{pmatrix} 0 & m_{23} & m_{31} & m_{12} \\ -m_{23} & 0 & m_{03} & m_{20} \\ -m_{31} & -m_{03} & 0 & m_{01} \\ -m_{12} & -m_{20} & -m_{01} & 0 \end{pmatrix} \tag{9}$$

with m_{ij} as defined in (2). Therefore $\mathtt{M}^*(\mathbf{u}, \mathbf{v})$ can be obtained from $\mathtt{M}(\mathbf{u}, \mathbf{v})$ by a certain interchange of coefficients by pairs, so that the mapping $\mathtt{M} \mapsto \mathtt{M}^*$ verifies $\mathtt{M}^{**} = \mathtt{M}$. Given the points $\mathbf{p}$, $\mathbf{q}$, the matrix $\mathtt{M}^*(\mathbf{p}, \mathbf{q})$ happens to be a Π-matrix of the line through them, and if $\boldsymbol{\alpha}$ and $\boldsymbol{\beta}$ are two planes, $\mathtt{M}^*(\boldsymbol{\alpha}, \boldsymbol{\beta})$ is a P-matrix of the line defined by them (A.1, P6).

Incidence between lines (A.1, P7) is easily established in terms of Plücker matrices. The line l_1 with P-matrix P_1 and the line l_2 with Π-matrix Π_2 intersect if and only if

$$\mathrm{trace}(\mathrm{P}_1\Pi_2) = 0. \tag{10}$$

In this case any non-zero column of the product $\mathrm{P}_1\Pi_2$ represents the intersection point and any non-zero row represents the common plane. In particular, for any P-matrix,

$$\mathrm{trace}(\mathrm{P}\mathrm{P}^*) = 0. \tag{11}$$

Note also that

$$4\det(\mathrm{P}) = \mathrm{trace}^2(\mathrm{P}\mathrm{P}^*) = \mathrm{trace}^2(\Pi\,\Pi^*) \tag{12}$$

so that condition (11) is equivalent to (5).

Consider the the linear mapping given by $\mathbf{p}' = \mathtt{H}\mathbf{p}$. The associated coordinate changes for P-matrices and Π-matrices derive from the following relationships (see A.1, P8)

$$\mathtt{M}(\mathbf{p}', \mathbf{q}') = \mathtt{H}\,\mathtt{M}(\mathbf{p}, \mathbf{q})\,\mathtt{H}^\top. \tag{13}$$

$$\mathtt{M}^*(\mathtt{H}\mathbf{p}, \mathtt{H}\mathbf{q}) = \det(\mathtt{H})\ \mathtt{H}^{-\top}\mathtt{M}^*(\mathbf{p}, \mathbf{q})\mathtt{H}^{-1}. \tag{14}$$

3.2. **Plücker coordinates.** A convenient choice of basis of the set of 4×4 antisymmetric matrices is

$$\begin{aligned} \mathsf{B} =& \{\mathtt{M}(\mathbf{e}_2, \mathbf{e}_3), \mathtt{M}(\mathbf{e}_0, \mathbf{e}_3), \mathtt{M}(\mathbf{e}_1, \mathbf{e}_3), \mathtt{M}(\mathbf{e}_2, \mathbf{e}_0), \mathtt{M}(\mathbf{e}_1, \mathbf{e}_2), \mathtt{M}(\mathbf{e}_0, \mathbf{e}_1)\} = \\ & \{\mathtt{M}^*(\mathbf{e}_0, \mathbf{e}_1), \mathtt{M}^*(\mathbf{e}_1, \mathbf{e}_2), \mathtt{M}^*(\mathbf{e}_2, \mathbf{e}_0), \mathtt{M}^*(\mathbf{e}_1, \mathbf{e}_3), \mathtt{M}^*(\mathbf{e}_0, \mathbf{e}_3), \mathtt{M}^*(\mathbf{e}_2, \mathbf{e}_3)\}, \end{aligned} \tag{15}$$

so that an antisymmetric matrix $\mathtt{A} = (a_{ij})$ will have coordinates with respect to B given by

$$\boldsymbol{\ell}_{\mathtt{A}} = (a_{23}, a_{03}, a_{13}, a_{20}, a_{12}, a_{01})^\top. \tag{16}$$

Note that given antisymmetric matrices $\mathtt{A}$, $\mathtt{B}$, we have

$$\frac{1}{2}\operatorname{trace}(\mathtt{AB}) = \boldsymbol{\ell}_{\mathtt{A}}^\top \boldsymbol{\ell}_{\mathtt{B}}. \tag{17}$$

A nice property of this basis is that relation (9) can be written as

$$\boldsymbol{\ell}_{\mathtt{A}^*} = \Omega\,\boldsymbol{\ell}_{\mathtt{A}}, \quad \text{where } \Omega = \begin{pmatrix} 0&0&0&0&0&1\\ 0&0&0&0&1&0\\ 0&0&0&1&0&0\\ 0&0&1&0&0&0\\ 0&1&0&0&0&0\\ 1&0&0&0&0&0 \end{pmatrix}, \tag{18}$$

and, since $\Omega^2 = \mathtt{I}$, we also have $\boldsymbol{\ell}_{\mathtt{A}} = \Omega\,\boldsymbol{\ell}_{\mathtt{A}^*}$.

We define the *Plücker coordinates* of a line as the coordinates of its P-matrix with respect to B, so if a line l is given by points $\mathbf{p}$, $\mathbf{q}$ or by planes $\boldsymbol{\alpha}$, $\boldsymbol{\beta}$, its Plücker coordinates

$\boldsymbol{\ell}$ are

$$\boldsymbol{\ell} \sim \boldsymbol{\ell}_{\mathtt{M}(\mathbf{p},\mathbf{q})} \sim \boldsymbol{\ell}_{\mathtt{M}^*(\boldsymbol{\alpha},\boldsymbol{\beta})}. \tag{19}$$

Relations (17) and (18) allow for an easy translation of previous formulas involving Plücker matrices to the language of Plücker coordinates. In particular, according to (11), a non-zero vector $\boldsymbol{\ell} \in \mathbb{C}^6$ will correspond to the Plücker coordinates of some line if and only if

$$\boldsymbol{\ell}^\top \Omega\, \boldsymbol{\ell} = 0. \tag{20}$$

The quadric with matrix Ω is known as the *Klein quadric.*

The incidence relation (10) in terms of Plücker coordinates is given by

$$\frac{1}{2}\,\mathrm{trace}\,(\mathrm{P}_1\mathrm{P}_2^*) = \boldsymbol{\ell}_{\mathrm{P}_1}^\top \Omega\, \boldsymbol{\ell}_{\mathrm{P}_2} = 0, \tag{21}$$

due to (17) and (18). Therefore two lines intersect if and only if their Plücker coordinates are conjugate with respect to the Klein quadric.

Given vectors $\mathbf{u}$, $\mathbf{v}$ of $\mathbb{C}^4$, we define

$$\begin{aligned} \mathbf{u} \wedge \mathbf{v} = \boldsymbol{\ell}_{\mathtt{M}(\mathbf{u},\mathbf{v})} &= \begin{pmatrix} m_{23} & m_{03} & m_{13} & m_{20} & m_{12} & m_{01} \end{pmatrix}^\top, \\ \mathbf{u} \underset{*}{\wedge} \mathbf{v} = \boldsymbol{\ell}_{\mathtt{M}^*(\mathbf{u},\mathbf{v})} &= \begin{pmatrix} m_{01} & m_{12} & m_{20} & m_{13} & m_{03} & m_{23} \end{pmatrix}^\top \end{aligned} \tag{22}$$

where $m_{ij} = u_i v_j - u_j v_i$. It is immediate that these operations are antisymetric and bilinear. Thus, if $\boldsymbol{\alpha}, \boldsymbol{\beta}$ represent planes defining the line l through the points $\mathbf{p}, \mathbf{q}$, then $\mathbf{p} \wedge \mathbf{q} \sim \boldsymbol{\alpha} \underset{*}{\wedge} \boldsymbol{\beta}$ are the Plücker coordinates of l.

From (18) and (22) it follows that

$$\Omega\,(\mathbf{u} \wedge \mathbf{v}) = \mathbf{u} \underset{*}{\wedge} \mathbf{v}, \;\; \Omega\,(\mathbf{u} \underset{*}{\wedge} \mathbf{v}) = \mathbf{u} \wedge \mathbf{v}. \tag{23}$$

Changes of coordinates of $\mathbb{P}^3$ affect Plücker coordinates according to a relationship deriving from (13). The change of coordinates of $\mathbb{P}^3$ given by $\mathbf{p}' = \mathtt{H}\mathbf{p}$ induces the change of Plücker coordinates

$$\boldsymbol{\ell}_{\mathtt{M}(\mathtt{H}\mathbf{p},\mathtt{H}\mathbf{q})} = \tilde{\mathtt{H}}\,\boldsymbol{\ell}_{\mathtt{M}(\mathbf{p},\mathbf{q})}. \tag{24}$$

where

$$\tilde{\mathtt{H}} = (\mathbf{h}_2 \wedge \mathbf{h}_3 \;\; \mathbf{h}_0 \wedge \mathbf{h}_3 \;\; \mathbf{h}_1 \wedge \mathbf{h}_3 \;\; \mathbf{h}_2 \wedge \mathbf{h}_0 \;\; \mathbf{h}_1 \wedge \mathbf{h}_2 \;\; \mathbf{h}_0 \wedge \mathbf{h}_1) \tag{25}$$

(this formula and the following are proved in A.2). The matrices of this form have the important property

$$\tilde{\mathtt{H}}^\top \Omega \tilde{\mathtt{H}} = \det(\mathtt{H})\Omega. \tag{26}$$

Formula (26) holds true also for singular matrices. We also have the relationship

$$\tilde{\mathtt{H}}^\top = \widetilde{\mathtt{H}^\top}. \tag{27}$$

3.3. **Plücker coordinates and projections.** Let us consider a camera given by a projection matrix $\mathtt{P}$. To each point $\mathbf{x}$ of the image plane we can associate its back-projected line. This line has Plücker coordinates (see A.2)

$$\boldsymbol{\ell} = \mathcal{P}\mathbf{x} \;\text{ where }\; \mathcal{P} = (\boldsymbol{\pi}_2 \underset{*}{\wedge} \boldsymbol{\pi}_3 \; \boldsymbol{\pi}_3 \underset{*}{\wedge} \boldsymbol{\pi}_1 \; \boldsymbol{\pi}_1 \underset{*}{\wedge} \boldsymbol{\pi}_2). \tag{28}$$

Conversely, given the line $\boldsymbol{\ell}$ of space, its projection has coordinates

$$\mathbf{r} = \begin{pmatrix} (\boldsymbol{\pi}_2 \wedge \boldsymbol{\pi}_3)^\top \\ (\boldsymbol{\pi}_3 \wedge \boldsymbol{\pi}_1)^\top \\ (\boldsymbol{\pi}_1 \wedge \boldsymbol{\pi}_2)^\top \end{pmatrix} \boldsymbol{\ell}.$$

4. The absolute line quadric

4.1. **Introducing the absolute line quadric.** We recall that the dual absolute quadric (DAQ), $\mathtt{Q}^*_\infty$, can be seen as a mapping that assigns to each plane $\boldsymbol{\alpha}$ the point at infinity corresponding to its orthogonal vector $\mathbf{X} = \mathtt{Q}^*_\infty \boldsymbol{\alpha}$ [16]. The DAQ is given by a rank-three 4×4 symmetric matrix $\mathtt{Q}^*_\infty$. Let us consider a line l given by the planes $\boldsymbol{\alpha}$ and $\boldsymbol{\beta}$

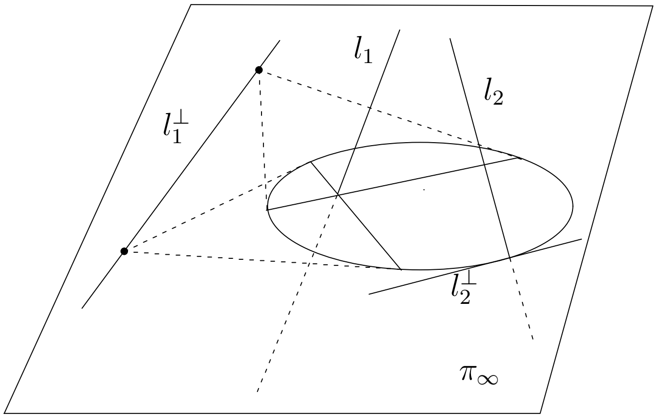

FIGURE 1. Incidence of lines with the absolute conic.

and not contained in the plane at infinity, $\boldsymbol{\pi}_\infty$. Then the line $l^\perp$ of $\boldsymbol{\pi}_\infty$ constituted by the orthogonal directions to l will be given by the points $\mathtt{Q}^*_\infty\boldsymbol{\alpha}$ and $\mathtt{Q}^*_\infty\boldsymbol{\beta}$. Therefore the P-matrix $\mathrm{P}^\perp$ of $l^\perp$ can be obtained as

$$\mathrm{P}^\perp = \mathtt{M}(\mathtt{Q}^*_\infty\boldsymbol{\alpha}, \mathtt{Q}^*_\infty\boldsymbol{\beta}) = \mathtt{Q}^*_\infty(\boldsymbol{\alpha}\boldsymbol{\beta}^\top - \boldsymbol{\beta}\boldsymbol{\alpha}^\top)\mathtt{Q}^*_\infty = \mathtt{Q}^*_\infty\Pi\mathtt{Q}^*_\infty. \tag{29}$$

where $\Pi = \mathtt{M}(\boldsymbol{\alpha}, \boldsymbol{\beta})$ is the Π-matrix of l.

Two lines l and l' are orthogonal if and only if $l^\perp$ intersects l', i.e., using (10), if

$$\operatorname{trace}(\Pi'\mathrm{P}^\perp) = \operatorname{trace}(\Pi'\mathtt{Q}^*_\infty\Pi\mathtt{Q}^*_\infty) = 0. \tag{30}$$

We recall that the line $l^\perp$ is the polar line with respect to the absolute conic of the point at infinity $\mathbf{p}_\infty$ of l. Therefore the lines that intersect the absolute conic are exactly those that intersect their own orthogonal line (see figure 1). We will call such lines *absolute lines*. Therefore absolute lines are characterized by the equation

$$\operatorname{trace}(\Pi\mathtt{Q}^*_\infty\Pi\mathtt{Q}^*_\infty) = \operatorname{trace}\left[(\Pi\mathtt{Q}^*_\infty)^2\right] = 0. \tag{31}$$

This is a quadratic expression in the coordinates of Π which will be called the *absolute line quadric* (ALQ).

The ALQ allows to express the Euclidean structure of space using Plücker matrices in an alternative way to the DAQ. In the same way as the DAQ is given by the tangent planes to the absolute conic, the ALQ is given by the set of lines that intersect it.

4.2. **The ALQ in terms of Plücker coordinates.** Note that (30) is a bilinear expression in Π and Π' that is also symmetric since the trace operator has the property $\mathrm{trace}(\mathtt{AB}) = \mathrm{trace}(\mathtt{BA})$ and therefore

$$\mathrm{trace}(\mathtt{A}_1\mathtt{A}_2\cdots\mathtt{A}_n) = \mathrm{trace}(\mathtt{A}_n\mathtt{A}_1\cdots\mathtt{A}_{n-1}) \tag{32}$$

whenever all the products make sense. Therefore some 6×6 symmetric matrix Σ exists so that

$$\frac{1}{2}\,\mathrm{trace}\left(\Pi'\mathtt{Q}^*_\infty\Pi\mathtt{Q}^*_\infty\right) = {\boldsymbol{\ell}'_{\Pi'^*}}^\top\Sigma\boldsymbol{\ell}_{\Pi^*}. \tag{33}$$

Hence two lines l and l', of Plücker coordinates $\boldsymbol{\ell} = \boldsymbol{\ell}_{\Pi^*}$ and $\boldsymbol{\ell}' = \boldsymbol{\ell}'_{\Pi'^*}$, are orthogonal if and only if

$${\boldsymbol{\ell}'}^\top\Sigma\boldsymbol{\ell} = 0. \tag{34}$$

Notice that

$$\begin{aligned} l' \perp l \Leftrightarrow& \\ {\boldsymbol{\ell}'}^\top\Sigma\boldsymbol{\ell} = 0 \Leftrightarrow& \text{ (since } \Omega^2 = \mathtt{I}) \\ {\boldsymbol{\ell}'}^\top\Omega(\Omega\Sigma\boldsymbol{\ell}) = 0 \Leftrightarrow& \text{ (using incidence condition (21))} \\ l' \text{ intersects } \Omega\Sigma\boldsymbol{\ell}&. \end{aligned} \tag{35}$$

Therefore $\Omega\Sigma\boldsymbol{\ell}$ are the Plücker coordinates of the line $l^\perp$ of orthogonal directions to l. As $l^\perp$ can be any line of the plane at infinity and since the vectors of the canonical basis of $\mathbf{C}^6$ are Plücker coordinates of lines, we conclude that the columns of $\Omega\Sigma$ are also Plücker coordinates of lines that span the lines contained in $\boldsymbol{\pi}_\infty$. In particular the columns of $\Omega\Sigma$ verify relation (20) or, equivalently, Σ verifies

$$\Sigma\Omega\Sigma = \mathtt{0}, \tag{36}$$

since $\Omega^2 = \mathtt{I}$. Besides, we see that Σ is a rank-three matrix, since the lines of a plane constitute a linear subspace of $\mathbf{C}^6$ of dimension three.

These results show that the kernel of Σ consists in the set of lines contained in the plane at infinity. To check this, observe from (36) that $\Sigma\Omega\Sigma\boldsymbol{\ell} = 0$ for any $\boldsymbol{\ell}$. Since $\Omega\Sigma\boldsymbol{\ell}$ can be any line at $\boldsymbol{\pi}_\infty$, the result follows.

4.3. **Obtaining the ALQ from the DAQ.** To obtain an explicit expression for Σ in terms of the dual absolute quadric $\mathtt{Q}^*_\infty$ we observe that

$$\begin{aligned}
\tfrac{1}{2}\,\mathrm{trace}(\Pi'\mathtt{Q}^*_\infty\Pi\mathtt{Q}^*_\infty) \quad &= \quad (\text{defining } \mathrm{P} = \Pi^*,\ \mathrm{P}' = (\Pi')^*)\\
\tfrac{1}{2}\,\mathrm{trace}(\mathrm{P}'^*\mathtt{Q}^*_\infty\mathrm{P}^*\mathtt{Q}^*_\infty) \quad &= \quad (\text{using } (17))\\
\boldsymbol{\ell}^\top_{\mathrm{P}'^*}\,\boldsymbol{\ell}_{\mathtt{Q}^*_\infty\mathrm{P}^*\mathtt{Q}^*_\infty}.&
\end{aligned}$$

Substituting in this expression $\mathrm{P} = \mathtt{M}(\mathbf{e}_i, \mathbf{e}_j)^*$ and noting by $\mathbf{q}_i$ the columns of $\mathtt{Q}^*_\infty$ we obtain,

$$\begin{aligned}
\boldsymbol{\ell}^\top_{\mathrm{P}'^*}\,\boldsymbol{\ell}_{\mathtt{Q}^*_\infty\mathtt{M}(\mathbf{e}_i,\mathbf{e}_j)\mathtt{Q}^*_\infty} &= (\text{using } (13))\\
\boldsymbol{\ell}^\top_{\mathrm{P}'^*}\,\boldsymbol{\ell}_{\mathtt{M}(\mathbf{q}_i,\mathbf{q}_j)} &= (\text{using } (25))\\
\boldsymbol{\ell}^\top_{\mathrm{P}'^*}(\mathbf{q}_i \wedge \mathbf{q}_j) &= (\text{using } (18))\\
\boldsymbol{\ell}^\top_{\mathrm{P}'}\Omega(\mathbf{q}_i \wedge \mathbf{q}_j) &= (\text{using } (23))\\
\boldsymbol{\ell}^\top_{\mathrm{P}'}(\mathbf{q}_i \underset{*}{\wedge} \mathbf{q}_j)&.
\end{aligned} \tag{37}$$

Taking into account the order of the basis $\mathtt{B}$ given in (15), we conclude that the matrix Σ is given by

$$\Sigma = \begin{pmatrix} \mathbf{q}_0 \underset{*}{\wedge} \mathbf{q}_1 & \mathbf{q}_1 \underset{*}{\wedge} \mathbf{q}_2 & \mathbf{q}_2 \underset{*}{\wedge} \mathbf{q}_0 & \mathbf{q}_1 \underset{*}{\wedge} \mathbf{q}_3 & \mathbf{q}_0 \underset{*}{\wedge} \mathbf{q}_3 & \mathbf{q}_2 \underset{*}{\wedge} \mathbf{q}_3 \end{pmatrix} \tag{38}$$

or, defining $\widetilde{\mathtt{Q}^*_\infty}$ analogously to formula (25) and using (23),

$$\Sigma = \Omega\widetilde{\mathtt{Q}^*_\infty}\Omega, \tag{39}$$

where we have used that right-multiplication by Ω inverts the order of the columns. We have thus obtained the desired relations between the DAQ and the ALQ.

4.4. **The ALQ in different coordinate systems.** In Euclidean coordinates, since $\mathtt{Q}^*_\infty$ has the canonical form $(\mathtt{Q}^*_\infty)_0 = (\mathbf{e}_0, \mathbf{e}_1, \mathbf{e}_2, \mathbf{0})$, we have that Σ has the canonical form

$$\Sigma_0 = \begin{pmatrix} \mathtt{I}_{3\times 3} & \mathtt{0}_{3\times 3} \\ \mathtt{0}_{3\times 3} & \mathtt{0}_{3\times 3} \end{pmatrix}. \tag{40}$$

Observe that if $\Sigma \sim \Sigma_0$, the coordinates are Euclidean. To check this, note that by (35) we have three lines of the plane at infinity given by the three non-zero columns of the matrix $\Omega\Sigma_0$, and it is immediate to check that the plane containing this three lines is that of equation $T = 0$. Now we can obtain the equation of the absolute conic by imposing that the line through the point $\mathbf{p} = (0, 0, 0, 1)^\top$ and a point $\mathbf{q} = (X, Y, Z, 0)^\top$ belongs to the ALQ. According to (22) this line has Plücker coordinates $\boldsymbol{\ell} = \boldsymbol{\ell}_{\mathtt{M}(\mathbf{p},\mathbf{q})} = (-Z, -X, -Y, 0, 0, 0)$, so that the condition is

$$\boldsymbol{\ell}^\top \Sigma_0 \,\boldsymbol{\ell} = X^2 + Y^2 + Z^2 = 0. \tag{41}$$

Therefore the absolute conic has the canonical equations $X^2 + Y^2 + Z^2 = T = 0$ and thus the coordinate system is Euclidean.

Let $\mathbf{p}' = \mathtt{H}\mathbf{p}$ be a coordinate change in $\mathbb{P}^3$ and $\boldsymbol{\ell}' = \tilde{\mathtt{H}}\boldsymbol{\ell}$ the corresponding coordinate change between Plücker coordinates (25). Then, the ALQ being a quadric, its matrix changes according to the rule

$$\Sigma' = \tilde{\mathtt{H}}^\top \Sigma \tilde{\mathtt{H}}. \tag{42}$$

From this, (40) and (27) it follows that if $\mathtt{H}$ is the matrix of a coordinate change from the current coordinate system to an Euclidean coordinate system, the ALQ Σ in the current coordinate system can be decomposed as

$$\Sigma = \begin{pmatrix} \mathbf{g}_2 \wedge \mathbf{g}_3 & \mathbf{g}_0 \wedge \mathbf{g}_3 & \mathbf{g}_1 \wedge \mathbf{g}_3 \end{pmatrix} \begin{pmatrix} \mathbf{g}_2 \wedge \mathbf{g}_3 & \mathbf{g}_0 \wedge \mathbf{g}_3 & \mathbf{g}_1 \wedge \mathbf{g}_3 \end{pmatrix}^\top. \tag{43}$$

where the $\mathbf{g}_i$ are the rows of $\mathtt{H}$. It is in this form that the matrix Σ was introduced in [11, Lemma 3], where it was interpreted as the matrix establishing orthogonality between lines.

4.5. **A linear constraint on the ALQ.** The coefficients of the ALQ verify the linear constraint given by $\mathrm{trace}(\Omega\Sigma) = 0$. In fact,

$$\begin{aligned} & \mathrm{trace}(\Omega\Sigma) \\ \text{(using (40) and (42))} \quad &= \mathrm{trace}(\Omega\tilde{\mathtt{H}}^\top\Sigma_0\tilde{\mathtt{H}}) \\ \text{(using (32))} \quad &= \mathrm{trace}(\tilde{\mathtt{H}}\Omega\tilde{\mathtt{H}}^\top\Sigma_0) \\ \text{(using (27))} \quad &= \mathrm{trace}(\widetilde{\mathtt{H}^\top}^\top\Omega\widetilde{\mathtt{H}^\top}\Sigma_0) \\ \text{(using (26))} \quad &= \mathrm{trace}(\det(\mathtt{H}^\top)\Omega\Sigma_0) = 0. \end{aligned}$$

This reduces one degree of freedom in the linear space of symmetric matrices of order six in which the ALQ matrices lie.

4.6. **Angle between two lines.** The angle $\theta \in [0, \pi/2]$ between two real lines of Plücker coordinates $\boldsymbol{\ell}$ and $\boldsymbol{\ell}'$ can be computed in terms of Σ as

$$\cos\theta = \frac{|\boldsymbol{\ell}^\top\Sigma\,\boldsymbol{\ell}'|}{\sqrt{(\boldsymbol{\ell}^\top\Sigma\,\boldsymbol{\ell})(\boldsymbol{\ell}'^\top\Sigma\,\boldsymbol{\ell}')}}. \tag{44}$$

It is enough to prove this formula for an Euclidean coordinate system. In these coordinates the intersection of the line $\boldsymbol{\ell}$ with the plane at infinity $x_3 = 0$ is, from equations (6) and (16),

$$\begin{pmatrix} 0 & l_5 & -l_3 & l_1 \\ l_5 & 0 & l_4 & l_2 \\ l_3 & -l_4 & 0 & l_0 \\ -l_1 & -l_2 & -l_0 & 0 \end{pmatrix} \begin{pmatrix} 0 \\ 0 \\ 0 \\ 1 \end{pmatrix} = \begin{pmatrix} l_1 \\ l_2 \\ l_0 \\ 0 \end{pmatrix}$$

so that the formula for the angle between two lines given their direction vectors $\mathbf{v} = (l_1, l_2, l_0)^\top$ and $\mathbf{v}' = (l_1', l_2', l_0')^\top$ becomes

$$\cos\theta = \frac{|\mathbf{v}^\top\mathbf{v}'|}{\sqrt{(\mathbf{v}^\top\mathbf{v})(\mathbf{v}'^\top\mathbf{v}')}} = \frac{|\boldsymbol{\ell}^\top\Sigma_0\,\boldsymbol{\ell}'|}{\sqrt{(\boldsymbol{\ell}^\top\Sigma_0\,\boldsymbol{\ell})(\boldsymbol{\ell}'^\top\Sigma_0\,\boldsymbol{\ell}')}}.$$

(cf. [11]).

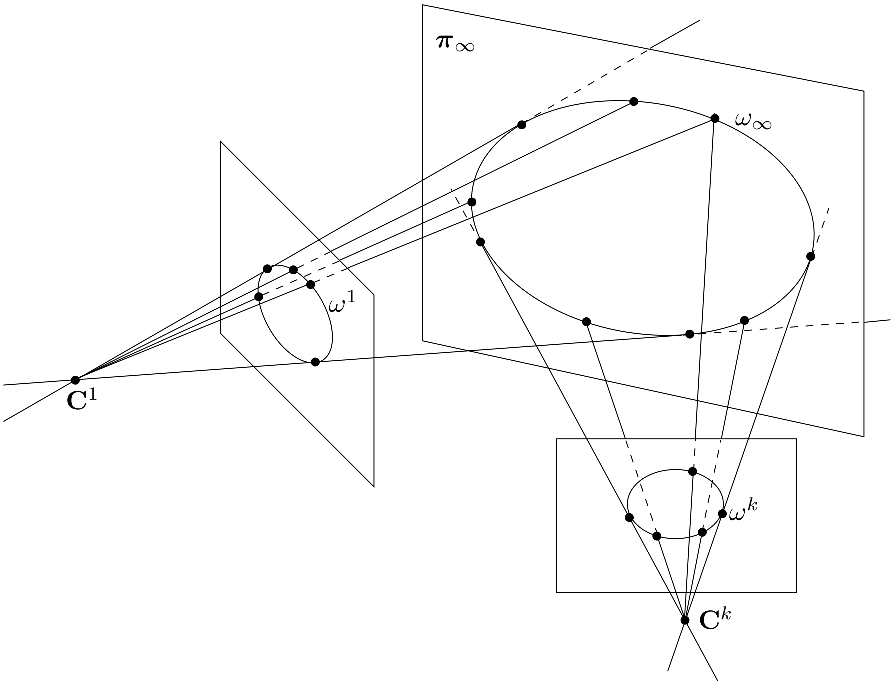

Figure 2. Obtaining the PAC from the ALQ.

4.7. **Computing the camera intrinsic parameters from Σ.**

4.7.1. *Projected absolute conic and intrinsic parameter matrix.* The projected absolute conic given by a projection $\mathtt{P}$ is the set of points of the projection plane whose back-projected lines intersect the absolute conic (see figure 2). Thus the matrix ω of the projected absolute conic can immediately be derived from Σ using (28) as

$$\omega = \mathcal{P}^\top \Sigma \mathcal{P}. \tag{45}$$

As is well known [5], the intrinsic parameter matrix can be retrieved from the projected absolute conic by Cholesky factorization from the relationship $\omega^* = \mathtt{K}\mathtt{K}^\top$, where $\omega^* \sim \omega^{-1}$ is the dual of the projected absolute conic.

Besides, some intrinsic parameters can be obtained explicitly, as we see in the following.

4.7.2. *Skew angle.* Since the skew angle θ of the camera is the angle between any two lines parallel to the coordinate retinal axes, it can be computed as the angle of the back-projected lines corresponding to the image points $(1, 0, 0)$ and $(0, 1, 0)$.

Considering the projection matrix $\mathtt{P}$ of rows $\boldsymbol{\pi}_i^\top$, $i = 1, 2, 3$, and combining equations (28) and (44) we obtain the formula

$$\cos\theta = \frac{|(\boldsymbol{\pi}_2 \underset{*}{\wedge} \boldsymbol{\pi}_3)^\top \Sigma\, (\boldsymbol{\pi}_3 \underset{*}{\wedge} \boldsymbol{\pi}_1)|}{\sqrt{[(\boldsymbol{\pi}_2 \underset{*}{\wedge} \boldsymbol{\pi}_3)^\top \Sigma\, (\boldsymbol{\pi}_2 \underset{*}{\wedge} \boldsymbol{\pi}_3)][(\boldsymbol{\pi}_3 \underset{*}{\wedge} \boldsymbol{\pi}_1)^\top \Sigma\, (\boldsymbol{\pi}_3 \underset{*}{\wedge} \boldsymbol{\pi}_1)]}}. \tag{46}$$

4.7.3. *Aspect ratio.* To compute the aspect ratio τ we observe that the image points of affine coordinates $(0, 0)$, $(1, 0)$, $(0, \tau)$, and $(1, \tau)$ are the vertices of a rhomb, so that its diagonals are orthogonal, and so are the back-projected lines of the points at infinity of these diagonals, $(1, \tau, 0)$ and $(1, -\tau, 0)$. So we have the relation

$$(1\ \tau\ 0)\mathcal{P}^\top \Sigma\, \mathcal{P} \begin{pmatrix} 1 \\ -\tau \\ 0 \end{pmatrix} = 0,$$

from which one obtains

$$\tau^2 = \frac{(\boldsymbol{\pi}_2 \underset{*}{\wedge} \boldsymbol{\pi}_3)^\top \Sigma (\boldsymbol{\pi}_2 \underset{*}{\wedge} \boldsymbol{\pi}_3)}{(\boldsymbol{\pi}_3 \underset{*}{\wedge} \boldsymbol{\pi}_1)^\top \Sigma (\boldsymbol{\pi}_3 \underset{*}{\wedge} \boldsymbol{\pi}_1)}. \tag{47}$$

Observe that the well-known conditions for the projection matrices of square-pixel cameras in Euclidean coordinates [4] are a particular case of (46) and (47) for $\theta = \pi/2$, $\tau = 1$, and $\Sigma = \Sigma_0$.

4.7.4. *Principal point.* The principal point $\mathbf{q}_0$ of the image is the image point whose back-projected line is orthogonal to the image plane. Taking for instance the directions $\mathbf{e}_0 = (1, 0, 0)^\top$ and $\mathbf{e}_1 = (0, 1, 0)^\top$, we have

$$\mathbf{q}_0^\top \mathcal{P}^\top \Sigma \mathcal{P} \mathbf{e}_i = 0,\ i = 0, 1,$$

so we have the explicit formula

$$\mathbf{q}_0 = (\mathcal{P}^\top \Sigma \mathcal{P} \mathbf{e}_0) \times (\mathcal{P}^\top \Sigma \mathcal{P} \mathbf{e}_1),$$

where × stands for the cross product in $\mathbf{C}^3$.

4.8. **Computing the DAQ from the ALQ.** Formula (38), giving the ALQ matrix Σ in terms of the DAQ matrix $\mathtt{Q}^*_\infty$ can be inverted by solving an homogeneous linear system of equations stemming from the following properties, that are immediate from relation (8):

$$\begin{aligned}\mathtt{M}^*(\mathbf{q}_i, \mathbf{q}_j)\mathbf{q}_i =& \mathbf{0}\\ \mathtt{M}^*(\mathbf{q}_i, \mathbf{q}_j)\mathbf{q}_k =& \mathtt{M}^*(\mathbf{q}_k, \mathbf{q}_i)\mathbf{q}_j.\end{aligned}$$

In our case the $\mathtt{M}^*$ matrices above can be built from the columns of Σ using formulas (38) and (22), and the right-multiplying $\mathbf{q}_l$ are the unknowns. The solution is obtained within the linear space of dimension ten of the symmetric 4×4 matrices and then approximated using a SVD decomposition by the closest rank-three symmetric matrix.

4.9. **Obtaining an Euclidean coordinate system from the ALQ.** Let $\mathtt{Q}^*_\infty$ and $(\mathtt{Q}^*_\infty)_0 = \operatorname{diag}(1, 1, 1, 0)$ be the matrices of the DAQ with respect to a projective and an Euclidean coordinate system, respectively. If $\mathtt{H}$ is any regular 4×4 matrix such that

$$\mathtt{Q}^*_\infty = \mathtt{H}(\mathtt{Q}^*_\infty)_0\mathtt{H}^\top \tag{48}$$

then $\mathtt{H}$ is indeed a matrix changing from an Euclidean coordinate system to the projective one (see [5, p. 447]). A practical way to find such a factorization is to compute a singular value decomposition (SVD) of $\mathtt{Q}^*_\infty$ so that

$$\mathtt{Q}^*_\infty = \mathtt{U}\operatorname{diag}(\sigma_0, \sigma_1, \sigma_2, 0)\mathtt{U}^\top \tag{49}$$

and, being necessarily all the $\sigma_i > 0$, define

$$\mathtt{H} = \mathtt{U}\operatorname{diag}(\sqrt{\sigma_0}, \sqrt{\sigma_1}, \sqrt{\sigma_2}, 1) \tag{50}$$

so that equation (48) holds true.

Regretably, if we are given the matrix Σ corresponding to a coordinate system arising from a projective coordinate system of $\mathbb{P}^3$ and a factorization

$$\Sigma = \mathtt{G}\Sigma_0\mathtt{G}^\top \tag{51}$$

with $\mathtt{G}$ a regular matrix, the matrix $\mathtt{G}$ does not even have to be the matrix $\tilde{\mathtt{H}}$ for any 4×4 regular matrix $\mathtt{H}$. To check this, observe that the last three columns of $\mathtt{G}$ are not determined by equation (51), and this freedom is not compatible with relation (26).

However, the factorization (51) does provide, according to the following theorem, that we prove in appendix A.4, the matrix of the change of coordinates to an Euclidean reference in an equally practical way.

Theorem 4.1. *We consider a factorization of the ALQ matrix of the form* $\Sigma = \mathtt{G}^T\Sigma_0\mathtt{G}$ *with* Σ_0 *as defined in (40) and* $\mathtt{G}^\top = (\mathbf{r}_0, \dots, \mathbf{r}_5)$*. Then the vectors* $\mathbf{r}_i$*,* $i = 0, 1, 2$*, can be written as* $\mathbf{r}_0 = \mathbf{v}_2 \wedge \mathbf{v}_3,\ \mathbf{r}_1 = \mathbf{v}_0 \wedge \mathbf{v}_3,\ \mathbf{r}_2 = \mathbf{v}_1 \wedge \mathbf{v}_3$ *for some linearly independent vectors* $\mathbf{v}_i$ *such that the matrix* $\mathtt{H}$ *given by* $\mathtt{H}^\top = (\mathbf{v}_0, \mathbf{v}_1, \mathbf{v}_2, \mathbf{v}_3)$ *gives a coordinate change from the current coordinate system to an Euclidean one.*

Therefore the vectors $\mathbf{v}_i$ are, seen as planes, the coordinates of the faces of an Euclidean coordinate tetrahedron. In particular, $\mathbf{v}_3$ is the plane at infinity. Hence the Plücker vectors $\Omega\,\mathbf{r}_0 = \mathbf{v}_2 \underset{*}{\wedge} \mathbf{v}_3, \Omega\,\mathbf{r}_1 = \mathbf{v}_0 \underset{*}{\wedge} \mathbf{v}_3, \Omega\,\mathbf{r}_2 = \mathbf{v}_1 \underset{*}{\wedge} \mathbf{v}_3$ represent the three lines of the plane at infinity of the Euclidean coordinate tetrahedron.

Observe that the decomposition $\Sigma = \mathtt{G}^\top\Sigma_0\mathtt{G}$ can be obtained by SVD followed by making zero the three lower singular values. The recovery of the vectors $\mathbf{v}_i$ from the $\mathbf{r}_i$ can be done as follows. We first obtain the P-matrices $\mathtt{M}_{kl}$ of the lines $\mathbf{r}_i$ by the conditions $\mathbf{r}_0 = \boldsymbol{\ell}_{\mathtt{M}_{23}}$, $\mathbf{r}_1 = \boldsymbol{\ell}_{\mathtt{M}_{03}}$ and $\mathbf{r}_2 = \boldsymbol{\ell}_{\mathtt{M}_{13}}$. Then we find $\mathbf{v}_3$ as a common vector in the kernel of the associated Π-matrices $\mathtt{M}^*_{i3}$, $i = 0, 1, 2$. To find the vectors $\mathbf{v}_i$, $i = 0, 1, 2$, we just take a vector in the orthogonal complement of $\mathbf{v}_3$ in the kernel of the corresponding Π-matrix $\mathtt{M}^*_{i3}$.

5. The absolute line quadric and cameras with known pixel shape

If the camera aspect ratio and skew are known, an affine coordinate transformation in the image permits to assume that the intrinsic parameters matrix has the form

$$\mathtt{K} = \begin{pmatrix} \alpha & 0 & u_0 \\ 0 & \alpha & v_0 \\ 0 & 0 & 1 \end{pmatrix}. \tag{52}$$

Let us consider the back-projected lines of image points $\mathbf{I} = (1, i, 0)^\top$, $\bar{\mathbf{I}} = (1, -i, 0)^\top$. We will term these lines the *isotropic lines* of the camera, as they correspond to the isotropic lines of the two-dimensional Euclidean vector space associated to the camera center and camera principal plane (see [3, p. 184]). These lines intersect the absolute conic, as we are going to see (figure 3). In fact, if $\mathbf{X} = (X, Y, Z, 0)^\top$ are the coordinates of the intersection of one of these two lines with the plane at infinity, we have

$$(1, \pm i, 0)^\top \sim \mathtt{P}\mathbf{X} = \mathtt{KR}(X, Y, Z)^\top,$$

so that

$$(X, Y, Z)^\top \sim \mathtt{R}^\top \mathtt{K}^{-1}(1, \pm i, 0)^\top,$$

and then

$$\begin{aligned} X^2 + Y^2 + Z^2 = (X, Y, Z)(X, Y, Z)^\top &= (1, \pm i, 0)\mathtt{K}^{-\top}\mathtt{RR}^\top\mathtt{K}^{-1}(1, \pm i, 0)^\top \\ &= \begin{pmatrix} 1 & \pm i \end{pmatrix} \begin{pmatrix} \alpha^{-2} & 0 \\ 0 & \alpha^{-2} \end{pmatrix} \begin{pmatrix} 1 \\ \pm i \end{pmatrix} = 0. \end{aligned}$$

Therefore, given a projective calibration of such cameras, two lines through the optical center belonging to the ALQ are known for each camera. According to equation (28), one of these lines has Plücker coordinates

$$\boldsymbol{\ell} = \mathcal{P}(1, i, 0)^\top = \boldsymbol{\pi}_2 \underset{*}{\wedge} \boldsymbol{\pi}_3 + i\,\boldsymbol{\pi}_3 \underset{*}{\wedge} \boldsymbol{\pi}_1 \tag{53}$$

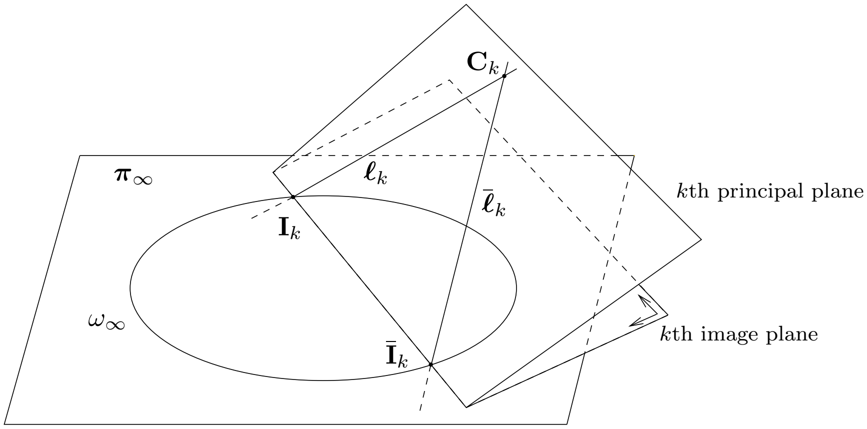

FIGURE 3. Intersections with the absolute conic of the isotropic lines of the camera k, with center $\mathbf{C}_k$.

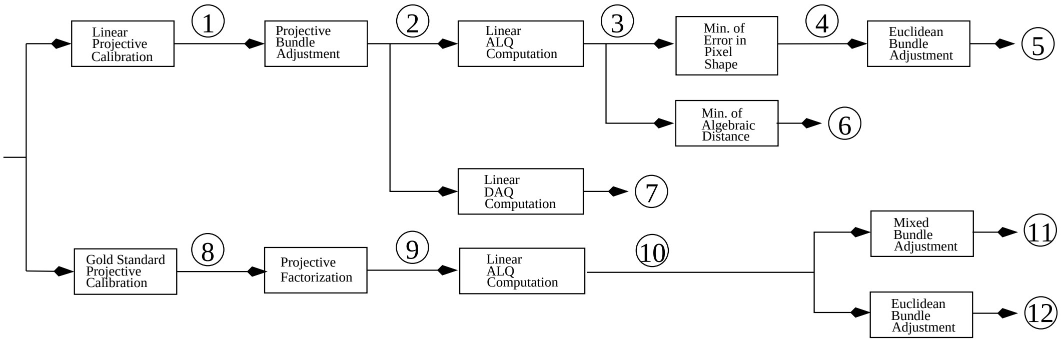
Linear Projective Calibration
1
Projective Bundle Adjustment
2
Linear ALQ Computation
3
Min. of Error in Pixel Shape
4
Euclidean Bundle Adjustment
5
Min. of Algebraic Distance
6
Linear DAQ Computation
7
Gold Standard Projective Calibration
8
Projective Factorization
9
Linear ALQ Computation
10
Mixed Bundle Adjustment
11
Euclidean Bundle Adjustment
12

FIGURE 4. Block diagram of the tested algorithms.

the other one being its complex conjugate, so that we have the relationship

$$
\begin{aligned}
&(\boldsymbol{\pi}_2 \underset{*}{\wedge} \boldsymbol{\pi}_3 + i\,\boldsymbol{\pi}_3 \underset{*}{\wedge} \boldsymbol{\pi}_1)^\top \Sigma(\boldsymbol{\pi}_2 \underset{*}{\wedge} \boldsymbol{\pi}_3 + i\,\boldsymbol{\pi}_3 \underset{*}{\wedge} \boldsymbol{\pi}_1) = \\
&(\boldsymbol{\pi}_2 \underset{*}{\wedge} \boldsymbol{\pi}_3)^\top \Sigma(\boldsymbol{\pi}_2 \underset{*}{\wedge} \boldsymbol{\pi}_3) - (\boldsymbol{\pi}_3 \underset{*}{\wedge} \boldsymbol{\pi}_1)^\top \Sigma(\boldsymbol{\pi}_3 \underset{*}{\wedge} \boldsymbol{\pi}_1) + \\
&\qquad 2i(\boldsymbol{\pi}_3 \underset{*}{\wedge} \boldsymbol{\pi}_1)^\top\ \Sigma(\boldsymbol{\pi}_2 \underset{*}{\wedge} \boldsymbol{\pi}_3) = 0.
\end{aligned}
\tag{54}
$$

Observe that the vanishing of the real and imaginary parts of this expression are in fact equivalent, respectively, to having aspect ratio $\tau = 1$ and having skew angle $\theta = \pi/2$, as follows from expressions (47) and (46).

As each camera provides a pair of linear equations in the coefficients of the ALQ, with ten cameras we obtain 20 linear equations which, together with the linear constraint given in subsection 4.5, provide Σ.

6. Algorithms

In this section we apply the previously developed theory to the design of algorithms for the Euclidean 3D reconstructions with uncalibrated cameras.

The proposed algorithms, based on the ALQ, are the following.

Linear ALQ Computation. This is the linear algorithm for the estimation of the ALQ given in section 5. It assumes square pixels and provides, using the technique in section 4.9, the rectifying homography $\mathtt{H}$ to convert a projective calibration of ten or more cameras into a Euclidean one.

Minimization of the Error in the Pixel Shape. This is a non-linear autocalibration algorithm to improve an initial rectifying homography by minimizing the cost function $g(\mathtt{H}) = \sum_{i=1}^{m} \left(|\epsilon_\theta^i(\mathtt{H})|^2 + |\epsilon_\tau^i(\mathtt{H})|^2\right)$ where $\epsilon_\theta^i(\mathtt{H}) = 1 - \theta(\mathtt{P}_i, \Sigma(\mathtt{H}))/\theta_i$, and $\epsilon_\tau^i(\mathtt{H}) = 1-\tau(\mathtt{P}_i, \Sigma(\mathtt{H}))/\tau_i$ are the relative errors in the θ and τ parameters respectively for camera i. Functions θ and τ are obtained from formulas (46) and (47). We compute $\Sigma(\mathtt{H}) = \tilde{\mathtt{H}}^\top \Sigma_0 \tilde{\mathtt{H}}$ according to (42). The optimization is achieved using a sparse Levenberg–Marquardt algorithm.

Minimization of the algebraic distance. This is a non-linear autocalibration algorithm that improves an initial rectifying homography by minimizing the cost function:

$$g(\mathtt{H}) = \sum_{k=1}^{m} \left| \frac{\boldsymbol{\ell}_k^\top \Sigma(\mathtt{H}) \boldsymbol{\ell}_k}{\|\boldsymbol{\ell}_k\|^2 \|\Sigma(\mathtt{H})\|_F} \right|^2 \tag{55}$$

where $\boldsymbol{\ell}_k$ is the back-projected line of the cyclic point $(1, i, 0)^\top$ for camera k.

Mixed Bundle Adjustment. This algorithm minimizes the cost function

$$g(\mathtt{P}_i, \mathbf{X}_j, \mathtt{H}) = \sum_{i,j=1}^{m,n} d(\mathtt{P}_i \mathbf{X}_j, \mathbf{x}_{ij})^2 + \xi \left(\sum_{i=1}^{m} |\epsilon_\theta^i(\mathtt{P}_i, \mathtt{H})|^2 + |\epsilon_\tau^i(\mathtt{P}_i, \mathtt{H})|^2 \right) \tag{56}$$

where ξ is a weighting factor that we set as $\xi = n^2$ and $\epsilon_\theta^i(\mathtt{P}_i, \mathtt{H}) = 1 - \theta(\mathtt{P}_i, \Sigma(\mathtt{H}))/\theta_i$ and $\epsilon_\tau^i(\mathtt{P}_i, \mathtt{H}) = 1 - \tau(\mathtt{P}_i, \Sigma(\mathtt{H}))/\tau_i$, with functions θ and τ deriving from formulas (46) and (47). We are assuming that the initial $\mathtt{P}_i$ and $\mathbf{X}_j$ are projective data and that the initial $\mathtt{H}$ has been obtained by a linear algorithm. Note that the cost function $g(\mathtt{P}_i, \mathbf{X}_j, \mathtt{H})$ is overparametrized, since the Euclidean variables $\hat{\mathtt{P}}_i = \mathtt{P}_i \mathtt{H}$ and $\hat{\mathbf{X}}_j = \mathtt{H}^{-1} \mathbf{X}_j$ should suffice.

However, the overparametrization has been found to produce slightly better numerical results.

In order to evaluate the performance of these algorithms they have been combined in different ways with standard modules. More specifically, we have implemented the block diagram in figure 4. Now we describe its remaining blocks.

Linear Projective Calibration. This block provides an initial projective calibration, given a set of n matched points across m views. The normalized 8-point algorithm [5, p. 265] is used to compute the fundamental matrix between two of the views. The projective calibration of these two cameras is used in the linear triangulation algorithm [5, p. 297] to compute the 3D points. The normalized linear algorithm for resection [5, p. 170] is then applied to obtain the projection matrices of the remaining cameras.

Gold Standard Projective Calibration. This block provides an initial projective calibration, given a set of n matched points across m views by first applying the Gold-Standard algorithm [5, p. 268] to two of the cameras and then resection for the other cameras [5, p. 170].

Projective Factorization. This algorithm improves a previously obtained projective calibration using matrix factorizations [5, p. 430].

Projective Bundle Adjustment. This algorithm improves a previously obtained projective calibration by minimizing the reprojection error of the 3D points across all views [5, p. 580].

Linear DAQ Computation. Linear algorithm for the estimation of the DAQ [5, p. 448] given three or more cameras. It assumes square pixels and principal point at the origin and provides the corresponding rectifying homography.

Euclidean Bundle Adjustment. This algorithm improves a previously obtained Euclidean calibration by minimizing the reprojection error of the 3D points across all views with respect to the camera calibration matrices $\mathtt{K}_i$, the positions of the cameras given by $\mathtt{R}_i$, $\mathbf{t}_i$ and the Euclidean 3D points $\mathbf{X}_j$. Square pixel conditions are enforced in the projection matrices. To initialize the algorithm, the projection matrices and 3D points available at point 2 of the diagram in figure 4 are corrected with the homography

$\mathtt{H}$ available at point 4. Then a QR factorization is applied to the first three columns of each projection matrix, producing the upper triangular matrices $\tilde{\mathtt{K}}_i$ and the rotation matrices $\mathtt{R}_i$. The initial intrinsic parameter matrix $\mathtt{K}_i$ for each camera is then obtained from $\tilde{\mathtt{K}}_i$ by enforcing the square pixel conditions, $\theta_i = \pi/2$ and $\tau_i = 1$.

The scheme has been tested with synthetic data in a series of experiments involving the reconstruction of a set of 100 points from their projections in 10 to 40 images taken with uncalibrated cameras with varying parameters. The 3D points lie close to the origin of coordinates of a Euclidean reference and the cameras are located at random positions lying approximately over a sphere centered at the origin and roughly pointing towards it, so that the set of projected points is approximately centered in the virtual CCD. Skew angle and aspect ratio are fixed at respective values $\pi/2$ and 1. Normalized focal length α is selected in each experiment at random with a uniform distribution centered at 2000 pixels with a maximum deviation of $\pm 10\%$ from this value. The principal point is obtained from a uniform distribution with support in the square $[\pm 400, \pm 300]$, to simulate a large variation. With these parameters the projected point coordinates have values within the range of a 1000×750 pixel image and, in each image, the points are contained inside a square of side 500 pixels.

For each camera configuration, Gaussian noise with standard deviation σ between 0 and 5 pixels is added to the point projection coordinates. This is the input of the linear projective calibration block in figure 4. The algorithms have been implemented in Matlab on a P4 machine at 2.4 GHz.

We first discuss the results for 15 cameras, shown in figure 5. The effect of varying the number of cameras will be provided later. Note that the algorithm given by node 12 (black line) is the slowest one and does not reach the optimal reprojection error. This could be expected, due to the high non-linearity of the model function in the Euclidean bundle adjustment, as the Levenberg–Marquardt algorithm relies on the assumption of a locally linear model function. Also note that the standard deviations of the reprojection errors are approximately proportional to the average errors.

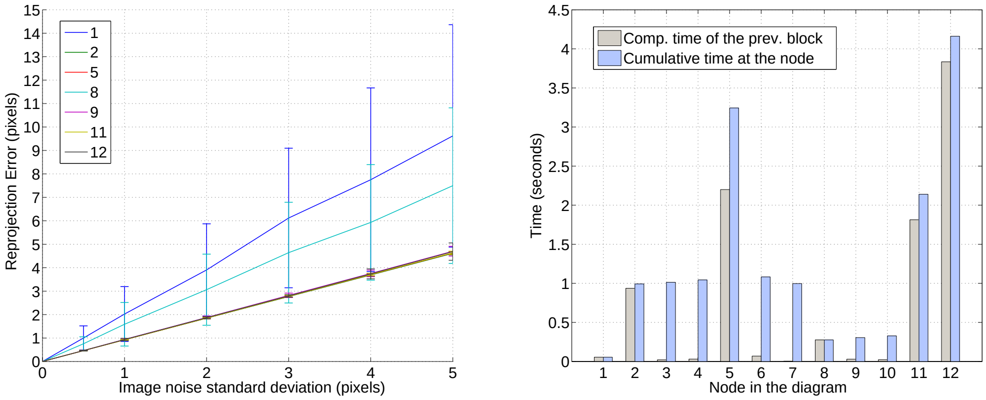

FIGURE 5. Results for 15 cameras. Left: average and standard deviation of the (residual) reprojection error of the tested algorithms. The numbers in the legend refer to the nodes in the block diagram of figure 4. Right: computation time required to reach each node and computation time spent in each block.

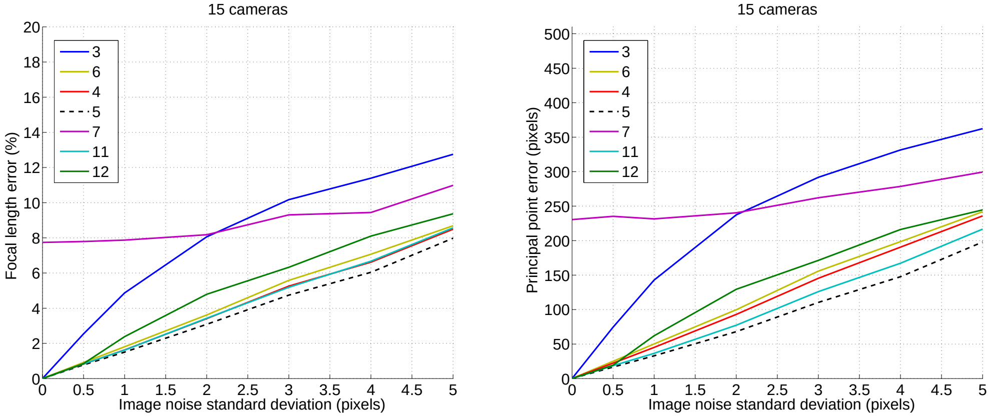

FIGURE 6. Errors in the estimation of the focal length (left) and the principal point (right) of the tested algorithms. The measured error in the principal point is the average of the Euclidean distances from the exact principal point to the estimated one. The numbers in the legend refer to the nodes in the block diagram of figure 4.

Figure 6 shows the errors in the estimation of the intrinsic parameters for 15 cameras. The linear ALQ algorithm gives overlapping error curves for nodes 3 and 10. Due to the large principal point deviation simulated, the linear DAQ algorithm is unable to provide good estimations for low noise levels as those that can be found in practice at this stage of the processing. The linear LAQ algorithm proves to be a suitable alternative. Considering all the linear and non-linear algorithms, it is seen that the best estimations are given by algorithms given by nodes 5 and 11. Their results are similar, but the computational cost of the later is lower.

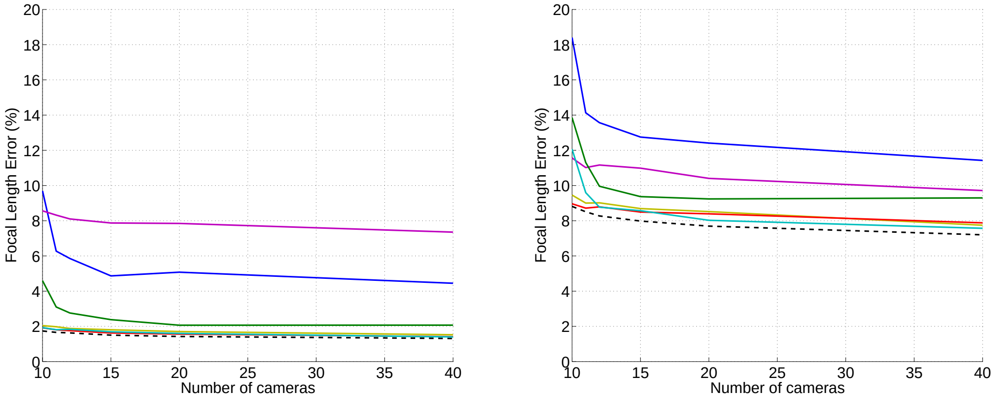

FIGURE 7. Errors in the estimation of the focal length of the tested algorithms as a function of the image noise and the number of cameras (color codes as in figure 6). Left: $\sigma = 1$. Right: $\sigma = 5$.

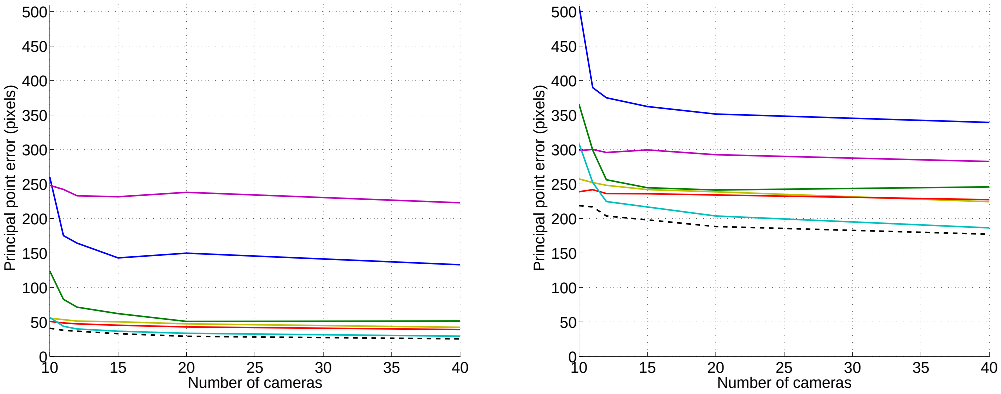

FIGURE 8. Errors in the estimation of the principal point of the tested algorithms as a function of the image noise and the number of cameras (color codes as in figure 6). Left: $\sigma = 1$. Right: $\sigma = 5$.

The results of the algorithm given by node 12 discourage from using the Euclidean bundle adjustment without an accurate initialization, since it might not reach an optimal solution in spite of a higher computational cost. Finally, observe that the results obtained in nodes 4 and 6 are quite similar.

Figures 7 and 8 show the influence of the number of cameras in the focal length and principal point errors, where an early saturation effect can be appreciated. The

Algorithm	Scene 1	Scene 2
Linear projective calibration	2.92	2.63
Gold Standard projective calibration	1.05	1.30
Projective bundle adjustment	0.55	0.48
Euclidean bundle adjustment	0.56	0.49
Mixed bundle adjustment	0.55	0.49

Table 1. RMS residual reprojection errors (pixels) for the experiments with real data.

computation time is not shown, as it is approximately proportional to the number of cameras.

7. Experiments with real data

In this section we presents the results of experiments with real data. For the reconstruction of the first scene (a set of books) 18 images of size 640 × 480 pixels where acquired with a digital camera. With a semiautomatic tool 76 points of the scene were matched accross the images, with an average of 56 points visible in each image.

A second experiment has consisted in the partial reconstruction of the Kings' courtyard of the monastery of El Escorial (Madrid, Spain). For this scene 23 images of 1024 × 768 were used, selecting 443 points, with an average of 372 simultaneously visible.

The matched points were taken as input of the algorithms summarized in figure 4. Due to the difficulty of using projective factorization with occluded points, this module has been substituted by the first iteration of the projective bundle adjustment. The residual RMS reprojection errors are shown in table 1.

From the projective bundle adjustment reprojection error the noise in the point positions is estimated respectively as $\sigma = 0.61$ pixels and 0.50 pixels. So the signal-to-noise ratio is of the order of 10^3, i.e., about four times the maximum considered in the simulations.

Figures 9 and 10 show respectively two views of the first and the second VRML reconstructed scenes corresponding to the algorithm of minimization of the error in the pixel shape.

Appendix A. Proofs

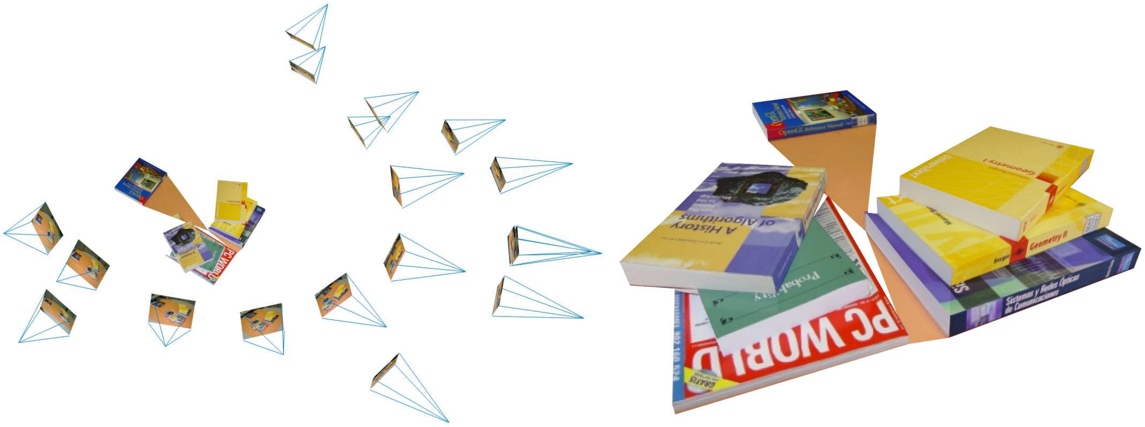

FIGURE 9. Two views of the first reconstructed 3D scene. The one on the left shows camera positions.

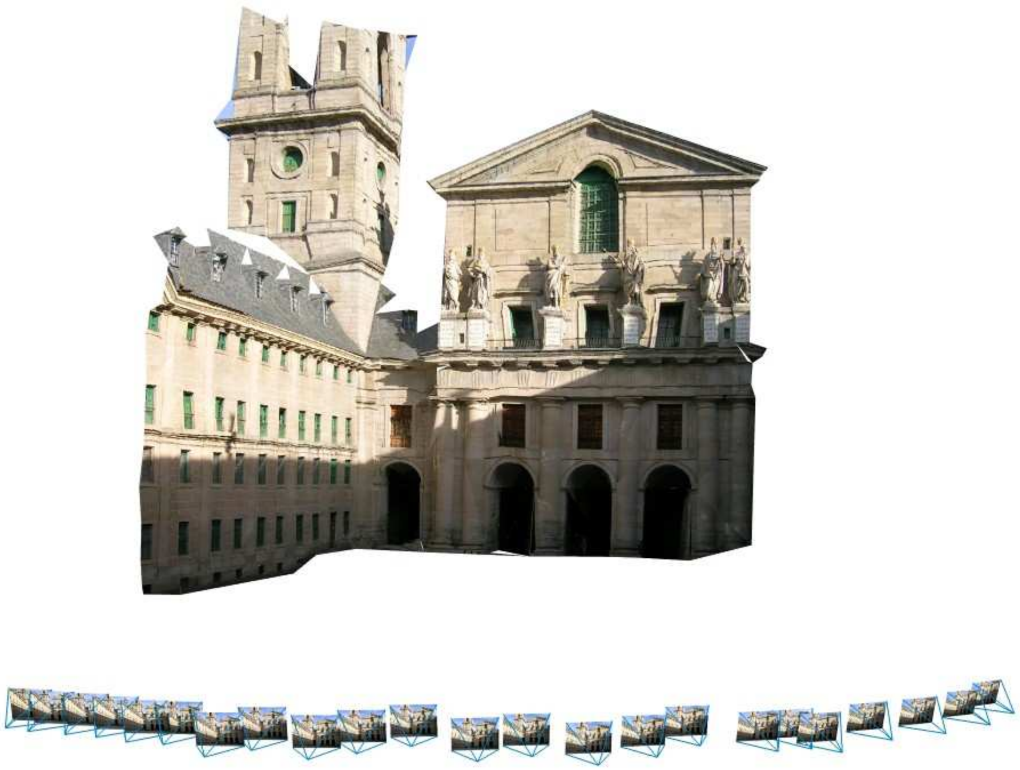

FIGURE 10. A view of the second reconstructed 3D scene (Kings' courtyard of El Escorial monastery, Madrid) showing camera positions.

A.1. **Properties of Plücker matrices.** As antisymmetric matrices are of even rank, a 4×4 antisymmetric matrix can only have rank zero, two, or four, so that non-null 4×4 singular antisymmetric matrices can only be of rank two. We state this explicitely for further reference.

Remark A.1. Non-null 4×4 singular antisymmetric matrices are of rank two.

Let $\mathtt{A}$ be a singular non-null antisymmetric matrix and let us take two different vectors $\mathbf{u}$ and $\mathbf{v}$ spanning its kernel. Let us consider a change of coordinates $\mathbf{p}' = \mathtt{H}\mathbf{p}$, so that $\mathbf{u}' = (1,0,0,0)$ and $\mathbf{v}' = (0,1,0,0)$. The antisymmetric matrix $\mathtt{A}' = \mathtt{H}^{-\top}\mathtt{A}\,\mathtt{H}^{-1}$ satisfies $\mathtt{A}'\mathbf{u}' = 0$, $\mathtt{A}'\mathbf{v}' = 0$, which imply that all the entries of $\mathtt{A}'$ vanish excepting $\mathtt{A}'_{3,4} = -\mathtt{A}'_{4,3}$. Therefore $\mathtt{A}'$ is defined up to a scalar factor and so is $\mathtt{A}$. So we have:

Remark A.2. A rank-two 4×4 antisymmetric matrix is determined by its kernel up to a proportionality constant.

Now we prove the properties of P-matrices stated in subsection 3.1. The corresponding properties of Π-matrices result from point-plane projective duality.

P1. P-matrices are of rank two: From the definition of a P-matrix $\mathrm{P} = \mathtt{M}(\mathbf{p},\mathbf{q})$, with $\mathbf{p},\mathbf{q}$ non-null and linearly independent, we see that its rank can be at most two, as the columns of the matrix are linear combinations of two vectors. So, from remark A.1, we just have to prove that P is not null. But since the columns of P are of the form $q_i\mathbf{p} - p_i\mathbf{q}$, if they were all zero, all the p_i and q_i coefficients would vanish, resulting in a contradiction.

P2. P-matrices are defined up to scale: Given any other pair of different points of the line $\bar{\mathbf{p}} = a\mathbf{p} + b\mathbf{q}$ and $\bar{\mathbf{q}} = c\mathbf{p} + d\mathbf{q}$, it is inmediate that their associated matrix $\bar{\mathrm{P}} = \mathtt{M}(\bar{\mathbf{p}},\bar{\mathbf{q}})$ equals $(ad - bc)\mathrm{P}$.

P3. The kernel of the P-matrix of a line is the pencil of planes containing the line: From the very definition of $\mathrm{P} = \mathtt{M}(\mathbf{p},\mathbf{q})$, any plane $\boldsymbol{\alpha}$ including the line clearly verifies $\mathrm{P}\boldsymbol{\alpha} = 0$. Being the kernel of P of dimension two, it must coincide with this pencil of planes.

P4. Necessary and sufficient condition for a matrix to be a P-matrix: Necessity of equation (5) derives from the singularity of the matrix. For the sufficiency, we first observe that, by remark A.1, the condition $\mathrm{P}\boldsymbol{\alpha} = 0$ defines a pencil of planes, and thus defines a line. Therefore we can compute the P-matrix of this line and obtain an antisymmetric matrix with the same kernel as P, and thus proportional to it by remark A.2.

P5. Intersection of line and plane: The point $\mathbf{X} = \mathrm{P}\boldsymbol{\alpha}$ belongs to the line with P-matrix P because its coordinates are a linear combination of the columns of P, which by its definition are points of the line. It is also included in the plane $\boldsymbol{\alpha}$ because, since P is antisymmetric, $\boldsymbol{\alpha}^\top \mathbf{X} = \boldsymbol{\alpha}^\top \mathrm{P}\boldsymbol{\alpha} = 0$.

P6. Obtainment of a P-matrix from two planes: Given the planes $\boldsymbol{\alpha}$, $\boldsymbol{\beta}$ that define the line l we consider the matrix $\mathtt{M}^*(\boldsymbol{\alpha}, \boldsymbol{\beta})$. From equation (8) it is clear that $\mathtt{M}^*(\boldsymbol{\alpha}, \boldsymbol{\beta})\boldsymbol{\gamma} = 0$ if and only if $\boldsymbol{\gamma}$ is another plane through l. Therefore $\mathtt{M}^*(\boldsymbol{\alpha}, \boldsymbol{\beta})$ is a P-matrix of l.

P7. Incidence between lines: Two lines l_1 and l_2, given by points $\mathbf{p}_1$, $\mathbf{q}_1$ and $\mathbf{p}_2$, $\mathbf{q}_2$ respectively, will intersect if and only if $\det(\mathbf{p}_1, \mathbf{q}_1, \mathbf{q}_2, \mathbf{p}_2) = 0$. But this determinant is, from (8), equal to

$$\begin{aligned}
&\mathbf{q}_2^\top \mathtt{M}^*(\mathbf{p}_1, \mathbf{q}_1)\mathbf{p}_2 = \mathrm{trace}(\mathbf{q}_2^\top \mathtt{M}^*(\mathbf{p}_1, \mathbf{q}_1)\mathbf{p}_2) \\
=&\frac{1}{2}\,\mathrm{trace}(\mathbf{q}_2^\top \mathtt{M}^*(\mathbf{p}_1, \mathbf{q}_1)\mathbf{p}_2 - \mathbf{p}_2^\top \mathtt{M}^*(\mathbf{p}_1, \mathbf{q}_1)\mathbf{q}_2) \\
=&\frac{1}{2}[\mathrm{trace}(\mathbf{q}_2^\top \mathtt{M}^*(\mathbf{p}_1, \mathbf{q}_1)\mathbf{p}_2) - \mathrm{trace}(\mathbf{p}_2^\top \mathtt{M}^*(\mathbf{p}_1, \mathbf{q}_1)\mathbf{q}_2)] \\
=&\frac{1}{2}[\mathrm{trace}(\mathtt{M}^*(\mathbf{p}_1, \mathbf{q}_1)\mathbf{p}_2\mathbf{q}_2^\top) - \mathrm{trace}(\mathtt{M}^*(\mathbf{p}_1, \mathbf{q}_1)\mathbf{q}_2\mathbf{p}_2^\top)] \\
=&\frac{1}{2}\,\mathrm{trace}(\mathtt{M}^*(\mathbf{p}_1, \mathbf{q}_1)\mathbf{p}_2\mathbf{q}_2^\top - \mathtt{M}^*(\mathbf{p}_1, \mathbf{q}_1)\mathbf{q}_2\mathbf{p}_2^\top) \\
=&\frac{1}{2}\,\mathrm{trace}(\mathtt{M}^*(\mathbf{p}_1, \mathbf{q}_1)\mathtt{M}(\mathbf{p}_2, \mathbf{q}_2))
\end{aligned}$$

where we have used the property of the trace operator (32). Therefore the line l_1 with P-matrix P_1 and the line l_2 with Π-matrix Π_2 intersect if and only if

$$\mathrm{trace}(\mathrm{P}_1\Pi_2) = 0. \tag{57}$$

If the two lines intersect, any non-zero column of the product $\mathrm{P}_1\Pi_2$ represents the intersection point, as a direct consequence of the fact that the columns of Π_2 represent planes containing l_2 and property P5 above. Analogously, any non-zero row of the product $\mathrm{P}_1\Pi_2$ represents the common plane. Finally we point out that, since a line intersects itself, clearly, for any P-matrix, $\mathrm{trace}(\mathrm{PP}^*) = 0$, but this condition is just (5).

P8. Changes of coordinates for the $\mathtt{M}$ and $\mathtt{M}^*$ operators: Consider the change of coordinates (or the linear mapping) in $\mathbb{P}^3$ given by $\mathbf{p}' = \mathtt{H}\mathbf{p}$. If the line l is defined by points $\mathbf{p}, \mathbf{q}$, its associated P-matrix will be given in the new coordinate system, according to (3) and (2), by

$$\mathtt{M}(\mathbf{p}', \mathbf{q}') = \mathtt{H}\,\mathtt{M}(\mathbf{p}, \mathbf{q})\,\mathtt{H}^\top. \tag{58}$$

Note that (58) is linear in $\mathtt{M}(\mathbf{p}, \mathbf{q})$. Analogously, the corresponding change of coordinates for planes $\boldsymbol{\alpha}' = \mathtt{H}^{-\top}\boldsymbol{\alpha}$ induces the associated formula for Π-matrices:

$$\mathtt{M}(\boldsymbol{\alpha}', \boldsymbol{\beta}') = \mathtt{M}(\mathtt{H}^{-\top}\boldsymbol{\alpha}, \mathtt{H}^{-\top}\boldsymbol{\beta}) = \mathtt{H}^{-\top}\mathtt{M}(\boldsymbol{\alpha}, \boldsymbol{\beta})\mathtt{H}^{-1}. \tag{59}$$

But since $\mathtt{M}^*(\mathbf{p}, \mathbf{q}) \sim \mathtt{M}(\boldsymbol{\alpha}, \boldsymbol{\beta})$ and $\mathtt{M}^*(\mathbf{p}', \mathbf{q}') \sim \mathtt{M}(\boldsymbol{\alpha}', \boldsymbol{\beta}')$,

$$\mathtt{M}^*(\mathbf{p}', \mathbf{q}') = \mathtt{M}^*(\mathtt{H}\mathbf{p}, \mathtt{H}\mathbf{q}) = \rho\,\mathtt{H}^{-\top}\mathtt{M}^*(\mathbf{p}, \mathbf{q})\mathtt{H}^{-1} \tag{60}$$

for some scalar ρ. This proportionality constant can be obtained as follows. From (8) we have

$$(\mathtt{H}\mathbf{x})^\top\mathtt{M}^*(\mathtt{H}\mathbf{p}, \mathtt{H}\mathbf{q})(\mathtt{H}\mathbf{y}) = \det(\mathtt{H}\mathbf{x}, \mathtt{H}\mathbf{p}, \mathtt{H}\mathbf{q}, \mathtt{H}\mathbf{y}) = \det(\mathtt{H})\det(\mathbf{x}, \mathbf{p}, \mathbf{q}, \mathbf{y})$$

for any $\mathbf{x}$, $\mathbf{y}$. And, from (60), the left-hand side of this last equation is

$$(\mathtt{H}\mathbf{x})^\top(\rho\mathtt{H}^{-\top}\mathtt{M}^*(\mathbf{p}, \mathbf{q})\mathtt{H}^{-1})(\mathtt{H}\mathbf{y}) = \rho\mathbf{x}^\top\mathtt{M}^*(\mathbf{p}, \mathbf{q})\mathbf{y} = \rho\det(\mathbf{x}, \mathbf{p}, \mathbf{q}, \mathbf{y}),$$

so that $\rho = \det(\mathtt{H})$, i.e.,

$$\mathtt{M}^*(\mathtt{H}\mathbf{p}, \mathtt{H}\mathbf{q}) = \det(\mathtt{H})\,\mathtt{H}^{-\top}\mathtt{M}^*(\mathbf{p}, \mathbf{q})\mathtt{H}^{-1}. \tag{61}$$

A.2. **Plücker coordinates and linear mappings.** Changes of coordinates of $\mathbb{P}^3$ affect Plücker coordinates according to a relationship deriving from (58). The change $\mathbf{p}' = \mathtt{H}\mathbf{p}$

induces the change of Plücker coordinates $\boldsymbol{\ell}_{\mathtt{M}(\mathbf{Hp},\mathbf{Hq})} = \tilde{\mathtt{H}}\,\boldsymbol{\ell}_{\mathtt{M}(\mathbf{p},\mathbf{q})}$. To obtain the k-th column of $\tilde{\mathtt{H}}$ we have to compute the new Plücker coordinates of the line with original Plücker coordinates given by the k-th element of the canonical basis of $\mathbf{C}^6$. Denoting by $\mathbf{h}_l$ the columns of $\mathtt{H}$ and using (22) we have that $\boldsymbol{\ell}_{\mathtt{M}(\mathtt{H}\mathbf{e}_i,\mathtt{H}\mathbf{e}_j)} = \boldsymbol{\ell}_{\mathtt{M}(\mathbf{h}_i,\mathbf{h}_j)} = \mathbf{h}_i \wedge \mathbf{h}_j = \tilde{\mathtt{H}}\,\boldsymbol{\ell}_{\mathtt{M}(\mathbf{e}_i,\mathbf{e}_j)}$. From this equation and (15), we obtain the columns of $\tilde{\mathtt{H}}$:

$$\tilde{\mathtt{H}} = \left(\mathbf{h}_2 \wedge \mathbf{h}_3 \;\; \mathbf{h}_0 \wedge \mathbf{h}_3 \;\; \mathbf{h}_1 \wedge \mathbf{h}_3 \;\; \mathbf{h}_2 \wedge \mathbf{h}_0 \;\; \mathbf{h}_1 \wedge \mathbf{h}_2 \;\; \mathbf{h}_0 \wedge \mathbf{h}_1\right). \tag{62}$$

The matrices of this form have the important property $\tilde{\mathtt{H}}^\top \Omega \tilde{\mathtt{H}} = \rho\Omega$. This is geometrically clear, since $\tilde{\mathtt{H}}$ maps Plücker coordinates onto Plücker coordinates so it must preserve Ω. However, a direct proof will also allow us to compute the scaling factor ρ. We observe from (25) that the entries of the matrix $\tilde{\mathtt{H}}^\top \Omega \tilde{\mathtt{H}}$ are of the form

$$\begin{aligned}
& (\mathbf{h}_i \wedge \mathbf{h}_j)^\top \Omega (\mathbf{h}_k \wedge \mathbf{h}_l) \\
\text{(eq. (23))} \quad &= (\mathbf{h}_i \wedge \mathbf{h}_j)^\top (\mathbf{h}_k \underset{*}{\wedge} \mathbf{h}_l) \\
\text{(eq. (22))} \quad &= \boldsymbol{\ell}^\top_{\mathtt{M}(\mathbf{h}_i,\mathbf{h}_j)} \boldsymbol{\ell}_{\mathtt{M}^*(\mathbf{h}_k,\mathbf{h}_l)} \\
\text{(eq. (17))} \quad &= \frac{1}{2}\,\mathrm{trace}(\mathtt{M}(\mathbf{h}_i,\mathbf{h}_j)\mathtt{M}^*(\mathbf{h}_k,\mathbf{h}_l)) \\
\text{(eq. (13) and (14))} \quad &= \frac{1}{2}\,\mathrm{trace}(\mathtt{H}\mathtt{M}(\mathbf{e}_i,\mathbf{e}_j)\mathtt{H}^\top \det(\mathtt{H})\mathtt{H}^{-\top}\mathtt{M}^*(\mathbf{e}_k,\mathbf{e}_l)\mathtt{H}^{-1}) \\
&= \det(\mathtt{H})\frac{1}{2}\,\mathrm{trace}(\mathtt{M}(\mathbf{e}_i,\mathbf{e}_j)\mathtt{M}^*(\mathbf{e}_k,\mathbf{e}_l)) \\
&= \det(\mathtt{H})(\mathbf{e}_i \wedge \mathbf{e}_j)^\top \Omega (\mathbf{e}_k \wedge \mathbf{e}_l).
\end{aligned}$$

Therefore

$$\tilde{\mathtt{H}}^\top \Omega \tilde{\mathtt{H}} = \det(\mathtt{H})\mathtt{I}^\top \Omega \mathtt{I} = \det(\mathtt{H})\Omega. \tag{63}$$

Note that the construction of the matrix $\tilde{\mathtt{H}}$ from $\mathtt{H}$ can be done regardless of the regularity of $\mathtt{H}$ and that a continuity argument shows that formula (63) holds true also for singular matrices.

We can obtain an interesting alternative formula for $\tilde{\mathtt{H}}$ using $\mathtt{M}^*$ matrices. We recall that, given a cooordinate change $\mathbf{p}' = \mathtt{H}\mathbf{p}$, the corresponding coordinate change for planes is $\boldsymbol{\alpha}' = \mathtt{H}^{-\top}\boldsymbol{\alpha}$, and the resulting coordinate change for Plücker coordinates will be

$$\boldsymbol{\ell}_{\mathtt{M}^*(\boldsymbol{\alpha}',\boldsymbol{\beta}')} = \boldsymbol{\ell}_{\mathtt{M}^*(\mathtt{H}^{-\top}\boldsymbol{\alpha},\mathtt{H}^{-\top}\boldsymbol{\beta})} = \hat{\mathtt{H}}\,\boldsymbol{\ell}_{\mathtt{M}^*(\boldsymbol{\alpha},\boldsymbol{\beta})}. \tag{64}$$

Note that the matrix $\tilde{\mathtt{H}}$ is proportional but not necessarily equal to $\hat{\mathtt{H}}$. In fact, we have

$$\begin{aligned}
& \boldsymbol{\ell}_{\mathtt{M}^*(\boldsymbol{\alpha}',\boldsymbol{\beta}')} = \boldsymbol{\ell}_{\mathtt{M}^*(\mathtt{H}^{-\top}\boldsymbol{\alpha},\mathtt{H}^{-\top}\boldsymbol{\beta})} \\
\text{(eq. (14))} \quad & = \boldsymbol{\ell}_{\det(\mathtt{H}^{-1})\,\mathtt{H}\,\mathtt{M}^*(\boldsymbol{\alpha},\boldsymbol{\beta})\,\mathtt{H}^\top} \\
& = \det(\mathtt{H}^{-1})\,\boldsymbol{\ell}_{\mathtt{H}\,\mathtt{M}^*(\boldsymbol{\alpha},\boldsymbol{\beta})\,\mathtt{H}^\top} \\
\text{(P6)} \quad & = \det(\mathtt{H}^{-1})\,\boldsymbol{\ell}_{\mathtt{H}\,\mu\mathtt{M}(\mathbf{p},\mathbf{q})\,\mathtt{H}^\top} \\
\text{(eq. (13))} \quad & = \det(\mathtt{H}^{-1})\boldsymbol{\ell}_{\mu\,\mathtt{M}(\mathtt{H}\mathbf{p},\mathtt{H}\mathbf{q})} \\
\text{(eq. (24))} \quad & = \det(\mathtt{H}^{-1})\tilde{\mathtt{H}}\,\boldsymbol{\ell}_{\mu\,\mathtt{M}(\mathbf{p},\mathbf{q})} \\
& = \det(\mathtt{H}^{-1})\tilde{\mathtt{H}}\,\boldsymbol{\ell}_{\mathtt{M}^*(\boldsymbol{\alpha},\boldsymbol{\beta})}.
\end{aligned}$$

A comparison with (64) leads to

$$\tilde{\mathtt{H}} = \det(\mathtt{H})\,\hat{\mathtt{H}}. \tag{65}$$

Equation (64) can be written as well as $\hat{\mathtt{H}}^{-1}\,\boldsymbol{\ell}_{\mathtt{M}^*(\boldsymbol{\alpha}',\boldsymbol{\beta}')} = \boldsymbol{\ell}_{\mathtt{M}^*(\mathtt{H}^T\boldsymbol{\alpha}',\mathtt{H}^T\boldsymbol{\beta}')}$. Therefore, denoting by $\mathbf{g}_i$ the rows of $\mathtt{H}$ and according to the basis definition in (15), we have that

$$\hat{\mathtt{H}}^{-1} = \left(\mathbf{g}_0 \underset{*}{\wedge} \mathbf{g}_1 \;\; \mathbf{g}_1 \underset{*}{\wedge} \mathbf{g}_2 \;\; \mathbf{g}_2 \underset{*}{\wedge} \mathbf{g}_0 \;\; \mathbf{g}_1 \underset{*}{\wedge} \mathbf{g}_3 \;\; \mathbf{g}_0 \underset{*}{\wedge} \mathbf{g}_3 \;\; \mathbf{g}_2 \underset{*}{\wedge} \mathbf{g}_3\right). \tag{66}$$

Using (63) we obtain $\tilde{\mathtt{H}}^\top = \det(\mathtt{H})\Omega\tilde{\mathtt{H}}^{-1}\Omega$, and from (65) and (23),

$$\tilde{\mathtt{H}}^\top = \Omega\hat{\mathtt{H}}^{-1}\Omega = \left(\mathbf{g}_2 \wedge \mathbf{g}_3 \;\; \mathbf{g}_0 \wedge \mathbf{g}_3 \;\; \mathbf{g}_1 \wedge \mathbf{g}_3 \;\; \mathbf{g}_2 \wedge \mathbf{g}_0 \;\; \mathbf{g}_1 \wedge \mathbf{g}_2 \;\; \mathbf{g}_0 \wedge \mathbf{g}_1\right), \tag{67}$$

where we have used that right-multiplying a matrix by Ω reverts the order of the columns of the matrix. Comparison of (67) with (62), yields $\tilde{\mathtt{H}}^\top = \widetilde{\mathtt{H}^\top}$ (cf. [2]).

A.3. **Plücker coordinates and projections.** Let us consider a camera given by a projection matrix $\mathtt{P}$. A point $\mathbf{X} \in \mathbb{P}^3$ belongs to the back-projected line of $\mathbf{x} = (u, v, w)^\top$ if and only if $\mathbf{x} \sim \mathtt{P}\mathbf{X}$. Denoting by $\boldsymbol{\pi}_i^\top$ the rows of $\mathtt{P}$, we have $(u, v, w) \sim (\boldsymbol{\pi}_1^\top\mathbf{X}, \boldsymbol{\pi}_2^\top\mathbf{X}, \boldsymbol{\pi}_3^\top\mathbf{X})$, so that

$$(u\boldsymbol{\pi}_2^\top - v\boldsymbol{\pi}_1^\top)\mathbf{X} = 0, \;\; (v\boldsymbol{\pi}_3^\top - w\boldsymbol{\pi}_2^\top)\mathbf{X} = 0, \;\; (u\boldsymbol{\pi}_3^\top - w\boldsymbol{\pi}_1^\top)\mathbf{X} = 0.$$

Hence the equations above define the pencil of planes associated to the back-projected line of $\mathbf{x}$, which is therefore defined by the planes $\boldsymbol{\alpha}_1 = u\boldsymbol{\pi}_2 - v\boldsymbol{\pi}_1$, $\boldsymbol{\alpha}_2 = v\boldsymbol{\pi}_3 - w\boldsymbol{\pi}_2$ and $\boldsymbol{\alpha}_3 = u\boldsymbol{\pi}_3 - w\boldsymbol{\pi}_1$. We have

$$\begin{aligned}
\boldsymbol{\alpha}_1 \underset{*}{\wedge} \boldsymbol{\alpha}_2 &= v[u(\boldsymbol{\pi}_2 \underset{*}{\wedge} \boldsymbol{\pi}_3) + v(\boldsymbol{\pi}_3 \underset{*}{\wedge} \boldsymbol{\pi}_1) + w(\boldsymbol{\pi}_1 \underset{*}{\wedge} \boldsymbol{\pi}_2)] \\
\boldsymbol{\alpha}_2 \underset{*}{\wedge} \boldsymbol{\alpha}_3 &= -w[u(\boldsymbol{\pi}_2 \underset{*}{\wedge} \boldsymbol{\pi}_3) + v(\boldsymbol{\pi}_3 \underset{*}{\wedge} \boldsymbol{\pi}_1) + w(\boldsymbol{\pi}_1 \underset{*}{\wedge} \boldsymbol{\pi}_2)] \\
\boldsymbol{\alpha}_1 \underset{*}{\wedge} \boldsymbol{\alpha}_3 &= u[u(\boldsymbol{\pi}_2 \underset{*}{\wedge} \boldsymbol{\pi}_3) + v(\boldsymbol{\pi}_3 \underset{*}{\wedge} \boldsymbol{\pi}_1) + w(\boldsymbol{\pi}_1 \underset{*}{\wedge} \boldsymbol{\pi}_2)]\,.
\end{aligned}$$

At least one of the $\underset{*}{\wedge}$ products above must be non-zero, for if the three $\boldsymbol{\alpha}_i \underset{*}{\wedge} \boldsymbol{\alpha}_j$ vanish, we will have $\boldsymbol{\alpha}_1 \sim \boldsymbol{\alpha}_2 \sim \boldsymbol{\alpha}_3$ and the back-projected line would not be well-defined. Hence $u(\boldsymbol{\pi}_2 \underset{*}{\wedge} \boldsymbol{\pi}_3) + v(\boldsymbol{\pi}_3 \underset{*}{\wedge} \boldsymbol{\pi}_1) + w(\boldsymbol{\pi}_1 \underset{*}{\wedge} \boldsymbol{\pi}_2)$ must be nonzero and are the Plücker coordinates we were looking for. Thus the mapping from image points to back-projected lines is given by equation $\boldsymbol{\ell} = \mathcal{P}\mathbf{x}$ where $\mathcal{P} = (\boldsymbol{\pi}_2 \underset{*}{\wedge} \boldsymbol{\pi}_3 \; \boldsymbol{\pi}_3 \underset{*}{\wedge} \boldsymbol{\pi}_1 \; \boldsymbol{\pi}_1 \underset{*}{\wedge} \boldsymbol{\pi}_2)$.

Given the space line $\boldsymbol{\ell}$, a point $\mathbf{x}$ of the image plane will belong to the projection of $\boldsymbol{\ell}$ if and only if its back-projected line $\mathcal{P}\mathbf{x}$ intersects $\boldsymbol{\ell}$, i.e., $(\mathcal{P}\mathbf{x})^\top \Omega \boldsymbol{\ell} = \mathbf{x}^\top \mathcal{P}^\top \Omega \boldsymbol{\ell} = 0$. Therefore, the projection of $\boldsymbol{\ell}$ has coordinates $\mathcal{P}^\top \Omega \boldsymbol{\ell}$, so that the matrix of the mapping from lines in space to their projections is $\mathcal{P}^\top \Omega$ (cf. [4, p. 183]).

A.4. **Proof of Theorem 4.1.**

Proof. We begin by proving that the $\mathbf{r}_i$ are the Plücker coordinates of three concurrent lines. If we define the matrix $\mathcal{R} = \begin{pmatrix} \mathbf{r}_0 & \mathbf{r}_1 & \mathbf{r}_2 \end{pmatrix}$, we have $\Sigma = \mathtt{G}^\top \Sigma_0 \mathtt{G} = \mathcal{R}\mathcal{R}^\top$. Therefore $\mathcal{R}$ must be a rank-three matrix, since so is Σ. From (36), we have $\Sigma \Omega \Sigma = \mathtt{G}^\top \Sigma_0 \mathtt{G} \Omega \, \mathtt{G}^\top \Sigma_0 \mathtt{G} = \mathtt{0}$, which, due to the regularity of $\mathtt{G}$ and the fact that $\Sigma_0 \mathtt{G} = (\mathcal{R}, \mathtt{0}_{6\times 3})^\top$, implies $\mathcal{R}^\top \Omega \, \mathcal{R} = \mathtt{0}$, so that for $i = 0, 1, 2$ we have $\mathbf{r}_i^\top \Omega \, \mathbf{r}_j = 0$. These relationships mean, according to (20) and (21), that the $\mathbf{r}_i$ represent Plücker coordinates of lines intersecting pairwise.

Therefore there are two possible geometrical configurations for the lines represented by the $\mathbf{r}_i$: either they are noncoplanar lines intersecting in a common point or they are three lines in a common plane pairwise intersecting in three different points. These two interpretations are mutually excludent due to the linear independence of the $\mathbf{r}_i$. To discriminate the actual configuration, we will make use of the fact that the kernel of Σ are the lines of a plane (the plane at infinity). Let us first observe that the kernel of $\Sigma\Omega$ consists exactly of those lines intersecting the three lines $\mathbf{r}_i$. To check this, take $\mathbf{s}$ to represent any line intersecting the $\mathbf{r}_i$, so that $\mathbf{r}_i^\top \Omega \mathbf{s} = \mathbf{0}$, $i = 0, 1, 2$. Therefore $\mathcal{R}^\top \Omega \mathbf{s} = \mathbf{0}$, and then $\mathcal{R}\mathcal{R}^\top \Omega \mathbf{s} = \Sigma\Omega\mathbf{s} = \mathbf{0}$, so $\mathbf{s} \in \ker(\Sigma\Omega)$. Since both $\ker(\Sigma\Omega)$ and our set of intersecting lines are linear spaces of the same dimension (being the latter either the set of lines through the common point or in the common plane), they coincide.

As $\ker\Sigma$ are the lines of a plane, $\ker(\Sigma\Omega) = \Omega\ker\Sigma$ is a star of lines through a point (23). Since these lines include the $\mathbf{r}_i$, we conclude that the $\mathbf{r}_i$ share a common point represented by a certain vector $\mathbf{v}_3$, as we wanted to prove. Let us take three vectors $\mathbf{v}_i$, $i = 0, 1, 2$, such that $\mathbf{r}_0 = \mathbf{v}_2 \wedge \mathbf{v}_3$, $\mathbf{r}_1 = \mathbf{v}_0 \wedge \mathbf{v}_3$, $\mathbf{r}_2 = \mathbf{v}_1 \wedge \mathbf{v}_3$. We define the matrix $\mathtt{H}^\top = (\mathbf{v}_0, \mathbf{v}_1, \mathbf{v}_2, \mathbf{v}_3)$ so we can write our factorization as

$$\Sigma = \mathcal{R}\mathcal{R}^\top = \begin{pmatrix} \mathbf{v}_2 \wedge \mathbf{v}_3 & \mathbf{v}_0 \wedge \mathbf{v}_3 & \mathbf{v}_1 \wedge \mathbf{v}_3 \end{pmatrix} \begin{pmatrix} \mathbf{v}_2 \wedge \mathbf{v}_3 & \mathbf{v}_0 \wedge \mathbf{v}_3 & \mathbf{v}_1 \wedge \mathbf{v}_3 \end{pmatrix}^\top = \tilde{\mathtt{H}}^\top \Sigma_0 \tilde{\mathtt{H}},$$

where formulas (27) and (25) have been used. Therefore $\mathtt{H}$ is the matrix of the change of basis to a Euclidean coordinate system. □

References

[1] L. Agapito, E. Hayman, I. Reid. Self-Calibration of Rotating and Zooming Cameras. *Int. J. Computer Vision* 45, pp. 107-127. 2001.

[2] A. Bartoli and P. Sturm, The 3D Line Motion Matrix and Alignment of Line Reconstructions, *Int. J. Computer Vision* 57 (3), pp. 159-178.

[3] M. Berger, *Geometry*, vol. 1. Springer, Germany, 1987.

[4] O. Faugeras, Q.-T. Luong, *The geometry of multiple images*, MIT Press, Cambrige, Massachusetts, 2001.

[5] R.I. Hartley and A. Zisserman, *Multiple View Geometry in Computer Vision.* Cambridge University Press, Cambridge, UK, 2000.

[6] E. E. Hemayed, A Survey of Camera Self-Calibration, IEEE AVSS '03.

[7] A. Heyden and K. Astrom, Euclidean reconstruction from image sequences with varying and unknown focal length and principal point. Proc. CVPR'97, Puerto Rico, 1997.

[8] A. Heyden and K. Astrom, Minimal conditions on intrinsic parameters for Euclidean reconstruction. Asian Conference on Computer Vision, Hong Kong, 1998.

[9] S. J. Maybank and O. Faugeras, A Theory of Self-Calibration of a Moving Camera. *Int. J. Computer Vision* 8, pp. 123-152. 1992.

[10] M. Pollefeys, R. Koch and L. van Gool. Self-calibration and metric reconstruction inspite of varying and unknown intrinsic camera parameters, *Int. J. Computer Vision*, vol. 32, no. 1, pp. 7–25, 1999.

[11] J. Ponce, On computing metric upgrades of projective reconstructions under the rectangular pixel assumption. Proc. SMILE 2000.

[12] J. Ponce, K. McHenry, T. Papadopoulo, M. Teillaud, and B. Triggs. On the Absolute Quadratic Complex and its Application to Autocalibration. Proceedings of the IEEE Conference on Computer Vision and Pattern Recognition, San Diego, CA, June 2005.

[13] H. Pottmann and J. Wallner, *Computational Line Geometry*, Springer Verlag, Heidelberg, 2001.

[14] J.G. Semple and G.T. Kneebone, *Algebraic Projective Geometry*, Oxford University Press, 1998.

[15] Y. Seo, A. Heyden, Auto-calibration from the orthogonality constraints, ICCV'00.

[16] W. Triggs, Auto-calibration and the absolute quadric. Proc. IEEE Conference on Computer Vision and Pattern Recognition, pages 609–614. 1997.

[17] A. Valdés and J.I. Ronda, Camera autocalibration and the calibration pencil. *J. Math. Imaging and Vision*, vol. 23, no. 2, pp. 167-174, Sept. 2005.

[18] A. Valdés, J.I. Ronda, G. Gallego, The absolute line quadric and camera autocalibration, *Int. J. Computer Vision* (in print).

Index Terms: Image processing and computer vision, digitization and image capture, camera calibration